Tennessee Valley Authority, Post Office Box 2000, Decatur, Alabama 35609-2000

September 2, 2008

TVA-BFN-TS-418
TVA-BFN-TS-431

10 CFR 50.90

U.S. Nuclear Regulatory Commission
ATTN: Document Control Desk
Mail Stop OWFN, P1-35
Washington, D. C. 20555-0001

Gentlemen:

In the Matter of	)	Docket Nos. 50-259
Tennessee Valley Authority	)	50-260
		50-296

BROWNS FERRY NUCLEAR PLANT (BFN) – UNITS 1, 2, AND 3 - TECHNICAL SPECIFICATIONS (TS) CHANGES TS-431 AND TS-418 – EXTENDED POWER UPRATE (EPU) – RESPONSE TO ROUND 19 REQUEST FOR ADDITIONAL INFORMATION (RAI) (TAC NOS. MD5262, MD5263, AND MD5264)

By letters dated June 28, 2004 and June 25, 2004 (ADAMS Accession Nos. ML041840109 and ML041840301), TVA submitted license amendment applications to the NRC for the EPU of BFN Unit 1 and BFN Units 2 and 3, respectively. The proposed amendments would change the operating licenses to increase the maximum authorized core thermal power level of each reactor by approximately 14 percent to 3952 megawatts.

On August 12, 2008, NRC staff issued a Round 19 RAI (ML082340002) regarding the EPU license amendment requests. Enclosure 1 to this letter provides the response to the Round 19 RAI. Portions of the response to RAIs EMCB.147 and EMCB.192/150 require additional research and analysis to fully provide the requested information. As discussed in the response to these RAIs in Enclosure 1, the remainder of the information will be provided by September 19, 2008.

Note that Enclosure 1 contains information that Continuum Dynamics, Inc. (CDI) considers to be proprietary in nature and subsequently, pursuant to 10 CFR 2.390(a)(4), CDI requests that such information be withheld from public disclosure. Enclosure 2 contains the redacted version of the proprietary enclosure with the CDI proprietary material removed, which is suitable for public disclosure. Enclosure 3 provides an affidavit from CDI supporting this request.

D030
NRR

TVA has determined that the additional information provided by this letter does not affect the no significant hazards considerations associated with the proposed TS changes. The proposed TS changes still qualify for a categorical exclusion from environmental review pursuant to the provisions of 10 CFR 51.22(c)(9).

No new regulatory commitments are made in this submittal. If you have any questions regarding this letter, please contact me at (256)729-2636.

I declare under penalty of perjury that the foregoing is true and correct. Executed on this 2nd day of September, 2008.

Sincerely,

FOR

D. T. Langley
Manager of Licensing
and Industry Affairs

Enclosures:

1. Response to Round 19 Request for Additional Information (RAI) (proprietary version)

2. Response to Round 19 Request for Additional Information (RAI) (non-proprietary version)

3. CDI Affidavit

Enclosures
cc (Enclosures):

State Health Officer
Alabama State Department of Public Health
RSA Tower - Administration
Suite 1552
P.O. Box 303017
Montgomery, Alabama 36130-3017

NRC Senior Resident Inspector
Browns Ferry Nuclear Plant
10833 Shaw Road
Athens, AL 35611-6970

Rebecca L. Nease, Branch Chief
U.S. Nuclear Regulatory Commission
Region II
Sam Nunn Atlanta Federal Center
61 Forsyth Street, SW, Suite 23T85
Atlanta, Georgia 30303-8931

Eva Brown, Project Manager
U.S. Nuclear Regulatory Commission
(MS 08G9)
One White Flint, North
11555 Rockville Pike
Rockville, Maryland 20852-2739

JEE:DAH
Enclosures
cc (w/o Enclosures):
G. P. Arent, EQB 1B-WBN
W. R. Campbell, Jr. LP 3R-C
S. M. Douglas, POB 2C-BFN
R. F. Marks, Jr., PAB 1C-BFN
D. C. Matherly, BFT 2A-BFN
L. E. Nicholson, BR 4X-C
R. G. West, NAB 2A-BFN
B. A. Wetzel, BR 4X-C
S. A. Vance, WT 6A-K
E. J. Vigluicci, ET 11A-K
NSRB Support, LP 5M-C
EDMS (with enclosures) WT CA–K

C:\Documents and Settings\dahousle\My Documents\EPU\RAI 19\RAI 19 Response Cover Letter 09-02.doc

ENCLOSURE 2

TENNESSEE VALLEY AUTHORITY
BROWNS FERRY NUCLEAR PLANT (BFN)
UNITS 1, 2, AND 3

TECHNICAL SPECIFICATIONS (TS) CHANGES TS-431 AND TS-418
EXTENDED POWER UPRATE (EPU)

RESPONSE TO ROUND 19 REQUEST FOR ADDITIONAL INFORMATION (RAI)

(NON-PROPRIETARY VERSION)

Attached is the non-proprietary version of the response to Round 19 RAI.

Background

The following provides a discussion of the current noise removal methodology utilized for BFN main steam line (MSL) strain gage data.

Current Methodology

Three separate signals are obtained from the MSL strain gages with the data acquisition system (DAS):

Current Licensed Thermal Power (CLTP) - This is the total signal at 100% power including the fluctuating pressure and noise.

Low Flow (LF) - This is the signal at low steam flow conditions and consists of mechanical and electrical noise.

Electrical interference check (EIC) - This signal is obtained by removing the strain gage excitation voltage. With the strain gage excitation voltage removed, no signal is generated from the strain gages and the signal consists of the noise floor of the DAS plus any electromagnetic interference in the plant picked up by the cables from the strain gages to the DAS.

Prior to removing the LF noise from the CLTP, the following sequence of filtering is performed for both the CLTP and LF data:

1. Spectral subtraction of EIC across the 2-250 Hz band. The EIC signal is generally larger than the DAS noise floor and smaller than the LF signal. When the EIC signal is the same for both the LF and CLTP plant conditions, this subtraction cancels out. For Unit 2, a separate EIC signal at LF conditions is not available and it is assumed to be the same as EIC at CLTP conditions (see the response to RAI EMCB.147).
2. Mean filtering (0 - 2 Hz) and bandstop filtering of identified noise frequencies such as alternating current (AC) line noise (seen as multiples of 60 Hz), Variable Frequency Drive (VFD) AC line noise which varies with recirculation pump speed (seen as multiples of 16 to 60 Hz) and recirculation system pump vane passing frequencies which are dependant on pump speed.
3. Coherence filtering in accordance with the algorithm given in Appendix D of CDI Report No. 05-28P, "Methodology to Predict Full Scale Steam Dryer Loads from In-Plant Measurements," (Enclosure 6 to the May 5, 2006 submittal, "Steam Dryer Stress Report") (ADAMS Accession No. ML061300436). This filtering reduces components of the signal that do not exhibit coherence between upper and lower strain gage arrays and, thus, are not the result of steam line acoustics.

After processing through these filters, the LF fluctuating pressure (mechanical and electrical noise) is spectrally subtracted from the CLTP fluctuating pressure (acoustical signal and noise) at the MSL inlets with the CLTP reduction limited to 3 decibel (dB).

$$CLTPC_n = CLTP_n \max\{0.5\,, 1 - |LF_n| / |CLTP_n|\}$$

where:

$CLTPC_n$ – Fourier coefficients of conditioned CLTP data

$CLTP_n$ – Fourier coefficients of CLTP data

LF_n – Fourier coefficients of low flow data

n = 1-4 denoting the main steam line inlets

Deriving Fluctuating Pressure Using Noise Subtraction

Removal of the LF data from the CLTP data provides a method to remove a portion of the noise from the full power signal. In basic terms, the CLTP signal consists of the fluctuating pressure at 100% power (which produces the actual load on the steam dryer) plus noise.

CLTP = fluctuating pressure + noise

This noise consists of both mechanical and electrical noise.

Noise = mechanical noise + electrical noise

The LF signal is taken at plant conditions where the fluctuating pressure in the steam lines due to acoustics and flow induced vibration (FIV) load on the dryers is small. Therefore, the LF signal is a measurement of the sum of the mechanical and electrical noise components.

LF = Noise = mechanical noise + electrical noise

The electrical noise is measured by the EIC signal which removes the component of the signal which represents strain. The EIC signal consists of the electrical noise induced in the strain gage cables and the existing noise floor on the DAS. The measurement of the DAS noise floor is discussed in the response to EMCB.181.

EIC = electrical noise + DAS noise floor

In order to determine the fluctuating pressure at 100% power that is related to FIV load on the steam dryer, the LF signal is subtracted from the CLTP signal after EIC is subtracted from both the CLTP and LF signals. Thus,

Fluctuating pressure = [CLTP - EIC] - [LF - EIC]

Expanding by the previously defined terms provides the following equation.

Fluctuating pressure =
(fluctuating pressure +mechanical noise + electrical noise + DAS noise floor) -
(mechanical noise + electrical noise + DAS Noise Floor)

Figures EMCB.181-1a through 1d for Unit 1 and Figures EMCB.147-1a through 1d for Unit 2 provide power spectral density (PSD) graphs which are referred to in the following discussion.

DAS Noise Floor

The noise floor associated with the DAS was determined in laboratory tests as described in the response to RAI EMCB.181. The DAS noise floor is common to the acquisition system and is the same in each of the figures.

EIC

The EIC signal is plotted for each MSL strain gage location on Units 1 and 2. As described above, the EIC signal consists of the DAS noise floor and electrical noise in the plant that is induced in the cables between the DAS and the strain gages. No signal is being measured at the strain gages since the excitation voltage has been removed for this measurement.

For example, EIC for BFN1 A Upper (top plot on Figure EMCB.181-1a) shows little electrical noise above the DAS noise floor, indicating that the cables for that set of strain gages do not pick up significant plant noise. EIC for BFN1 A Lower (bottom plot on Figure EMCB.181-1a) shows an observable increase over the DAS noise floor, indicating that a small amount of electrical interference is picked up by those cables across the frequency spectrum. Unit 2 EIC for BFN2 C Upper (top plot on Figure EMCB.147-1c) shows electrical noise above the DAS noise floor similar to Unit 1 below 80 Hz but increases with frequency above 80 Hz.

The increase in electrical noise in Unit 2 relative to Unit 1 is most likely caused by the close proximity of the electrical penetration for the MSL strain gage signals to the electrical power penetration for recirculation pump 2A relative to Unit 1. The MSL strain gage penetration for Unit 2 is adjacent to the recirculation pump 2A penetration, while the closest recirculation pump penetration to the Unit 1 strain gage penetration is approximately 20 feet (See Figures EMCB-1 and 2).

Mechanical Noise

Mechanical noise is picked up by the MSL strain gages and included in the signal to the DAS. The dynamic equipment inside the primary containment which could potentially generate background strain include:

- Rotating equipment
  - Recirculation system pumps
  - Drywell cooling fans
- Fluid noise through the reactor recirculation system
- Vibration modes of the steam piping which are not canceled by opposing strain gage pairs

Plant mechanical noise can be illustrated in the figures for Units 1 and 2. In these figures, the mechanical noise introduced by the plant is represented as the difference between the LF signal and the EIC signal. As described above, the LF signal consists of the mechanical and electrical noise with minimal acoustic pressure fluctuation.

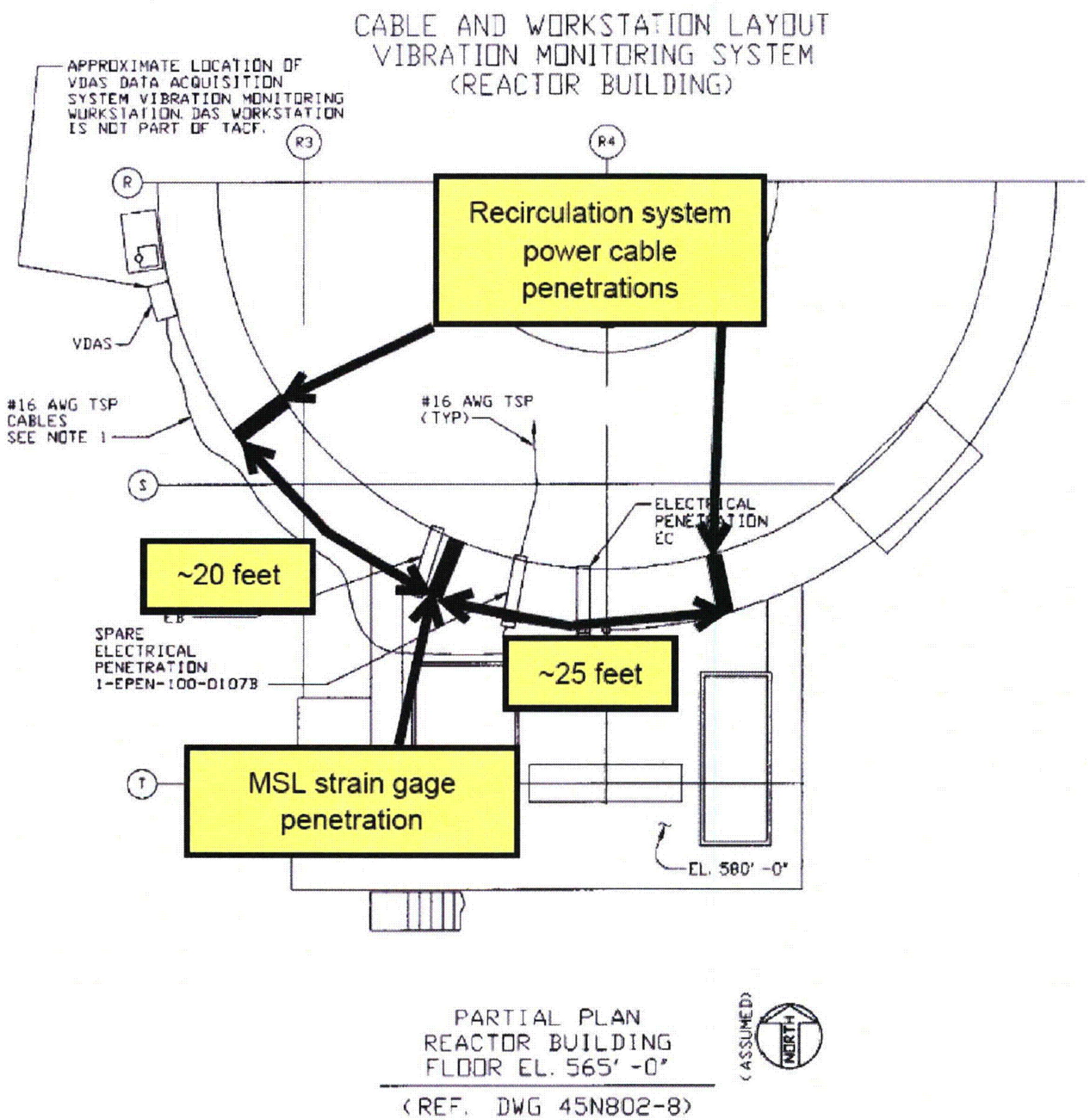

Figure EMCB-1: Unit 1 MSL Strain Gage Penetration

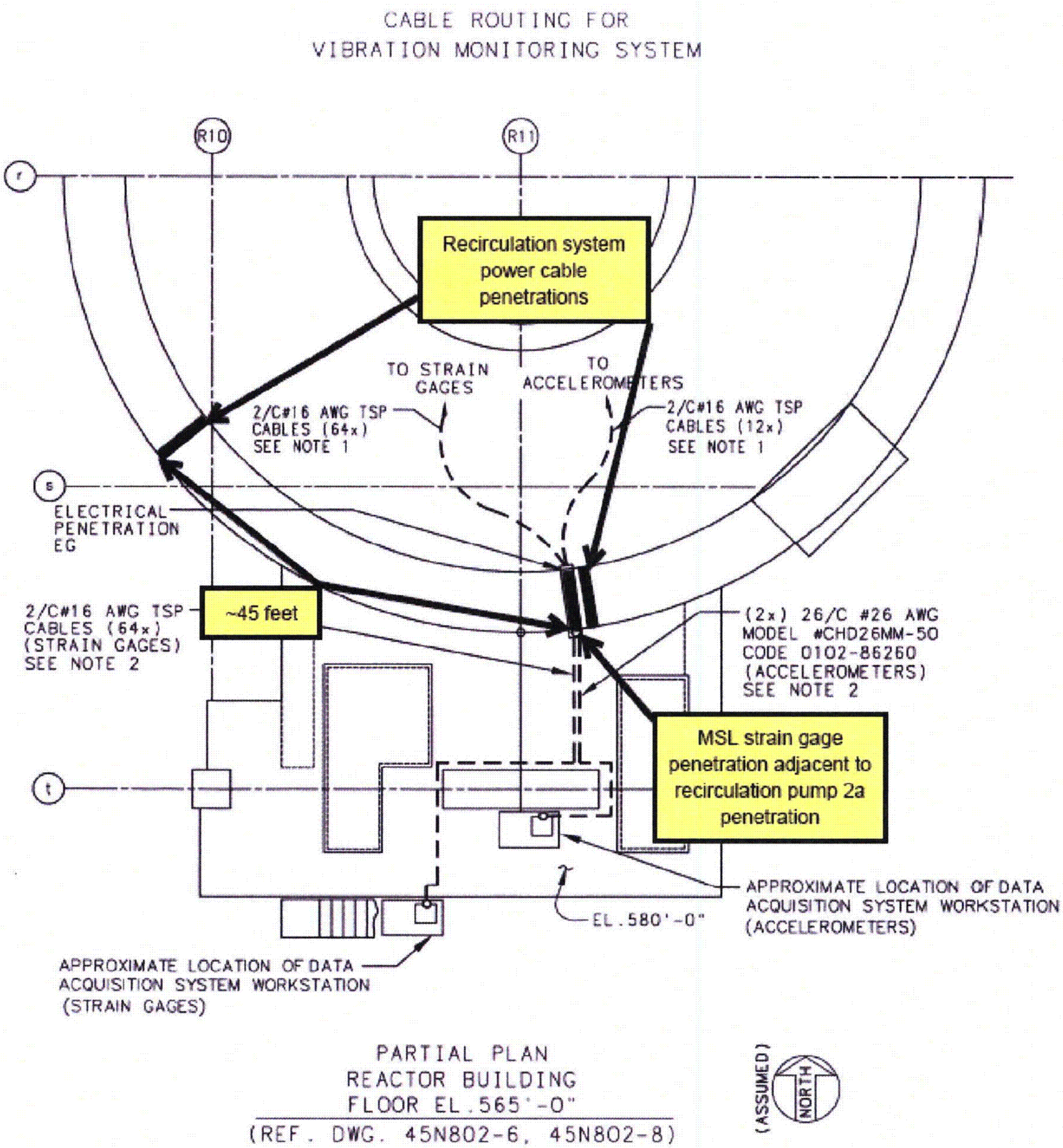

Figure EMCB-2: Unit 2 MSL Strain Gage Penetration

NRC RAI EMCB

In response to a Nuclear Regulatory Commission letter dated June 16, 2008, Tennessee Valley Authority (TVA) provided main steam line (MSL) strain gage power spectral densities (PSDs) for current licensed thermal power (CLTP) (without low-flow noise removal) and for low-flow conditions (9 percent reactor power) at each of the Browns Ferry Nuclear Plant (BFN) Unit 1 MSL strain gage locations. The licensee has indicated that the low-flow conditions signals are caused by plant background noise and, therefore, filters them from the corresponding signals at CLTP. Then the filtered data is used for the stress analysis of Unit 1 dryer. Given this discussion:

NRC RAI EMCB.181 (Unit 1 only)

Provide data and analysis to confirm that the Unit 1 low-flow signals are actually due to plant background noise events, and not the noise floors of the sensors and data acquisition systems.

TVA Response to EMCB.181 (Unit 1 only)

A DAS of the same type used at BFN was set up in a laboratory environment with cable and strain gages connected for the purpose of measuring the noise floor of the equipment itself. Figures EMCB.181-1a through 1e are PSD plots of the equipment noise floor as measured in the laboratory, the Unit 1 LF (9% power) data and the Unit 1 CLTP data. It can be seen that the plant noise data is well above the noise floor of the DAS and, therefore, is a valid measurement.

Figures EMCB.181-1a through 1d are PSD plots of Unit 1 signals which illustrate example signal magnitudes. The signals were filtered at the following frequencies to eliminate known noise sources.

CLTP

Frequency Range (Hz)	Filtering
0 - 2	Mean
59.8 - 60.2	Line Noise
119.9 - 120.1	Line Noise
179.8 - 180.2	Line Noise
239.9 - 240.1	Line Noise
50.5 - 51.5	VFD (1x)
127 - 128	Recirc Pumps A, B Speed (5x)
217 - 220	Standpipe Excitation

9% Power

Frequency Range (Hz)	Filtering
0 - 2	Mean
59.8 - 60.2	Line Noise
119.9 - 120.1	Line Noise
179.8 - 180.2	Line Noise
239.9 - 240.1	Line Noise
39 - 40	Recirc Pumps A, B Speed (5x)

EIC

Frequency Range (Hz)	Filtering
0 - 2	Mean
59.8 - 60.2	Line Noise
119.9 - 120.1	Line Noise
179.8 - 180.2	Line Noise
239.9 - 240.1	Line Noise
50.5 - 51.5	VFD (1x)

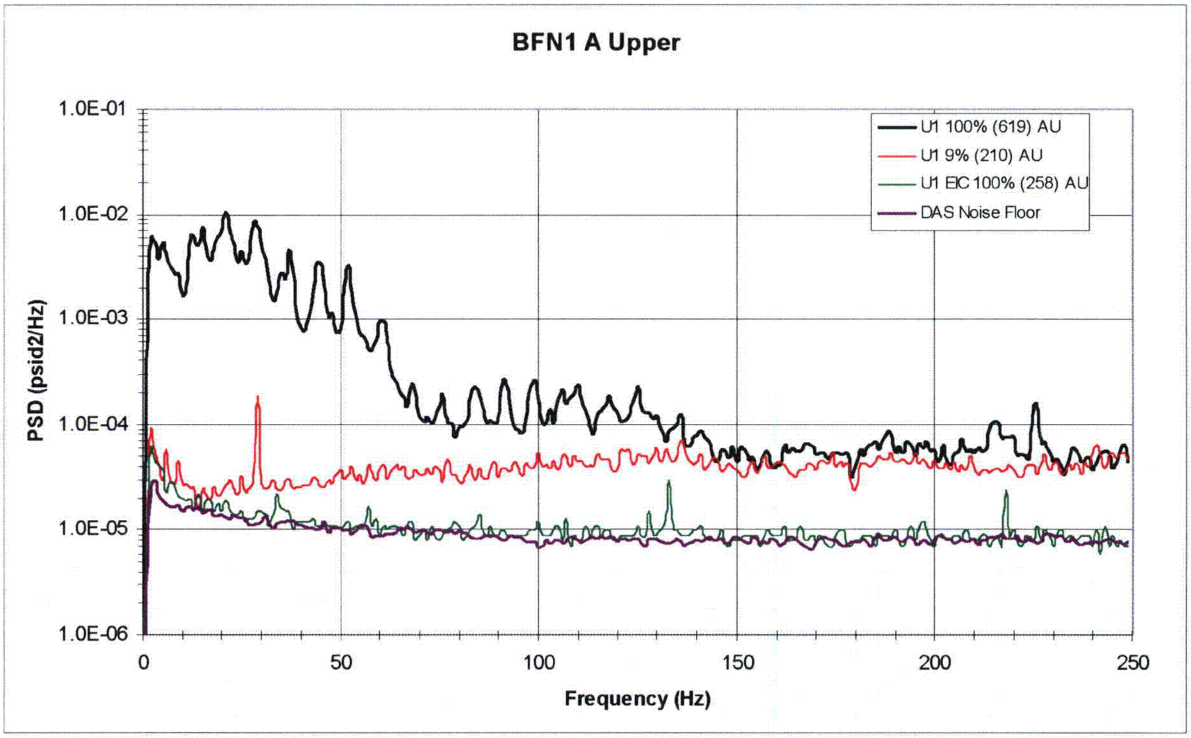

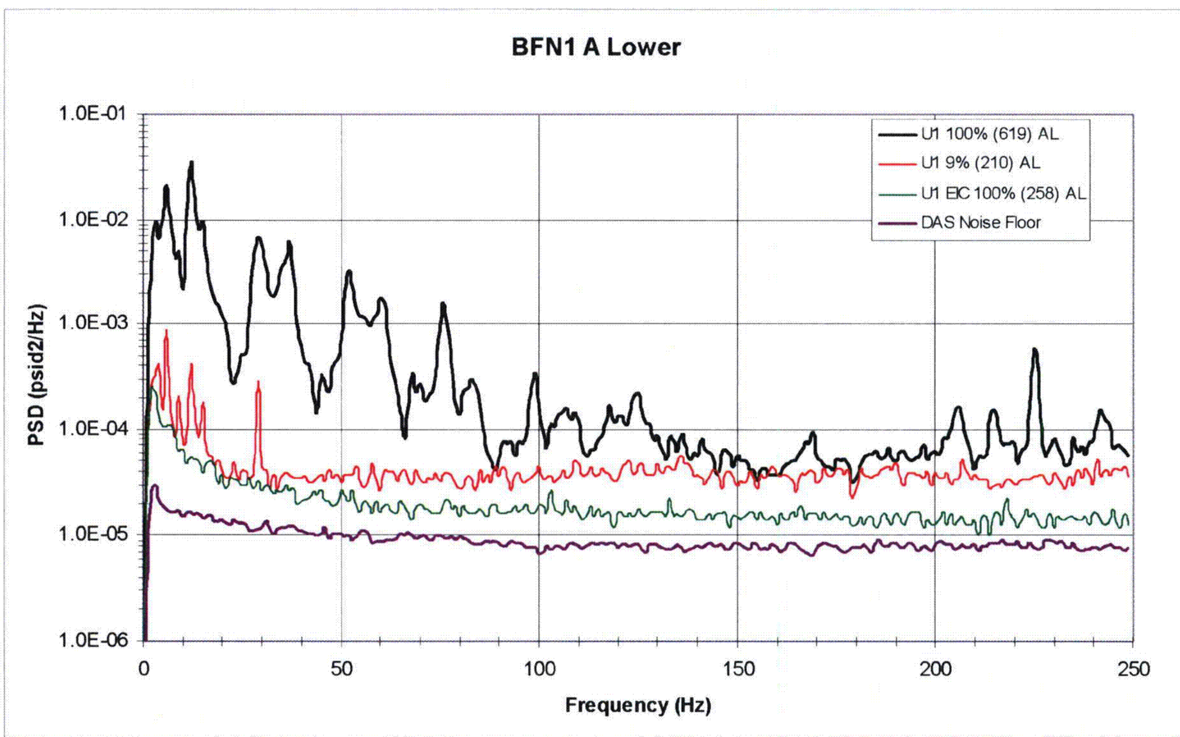

Figure EMCB.181-1a: Unit 1 Data MSL A

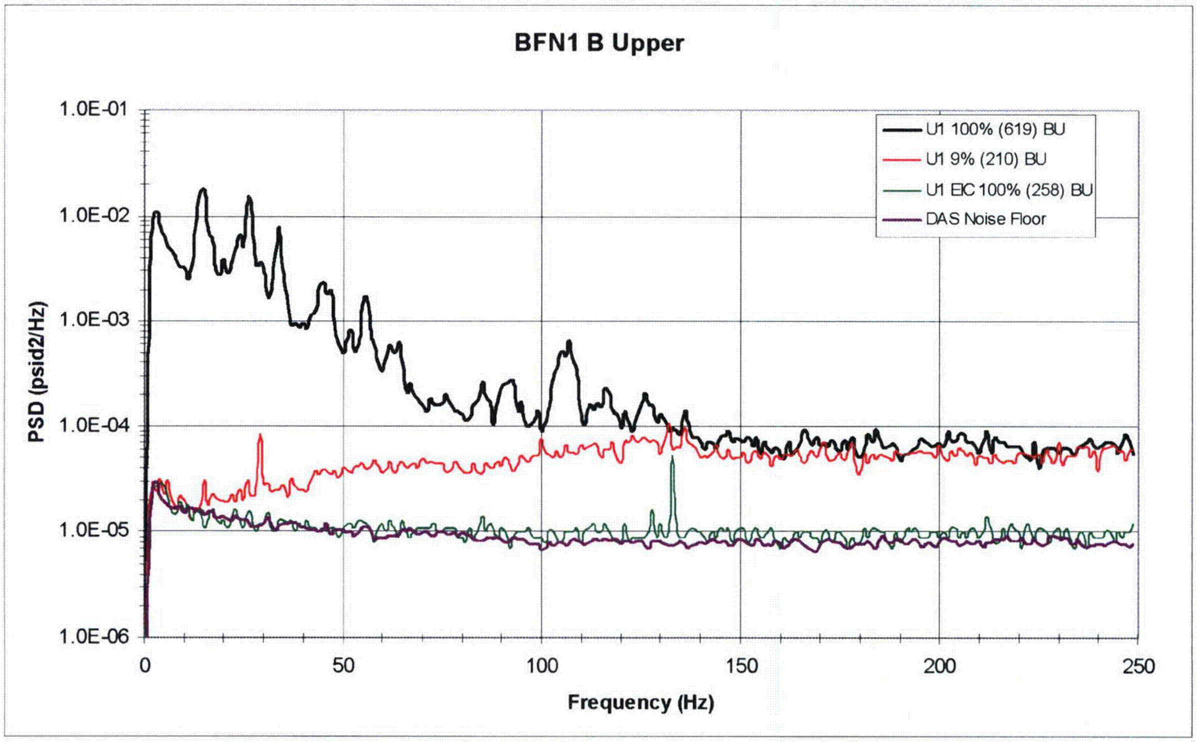

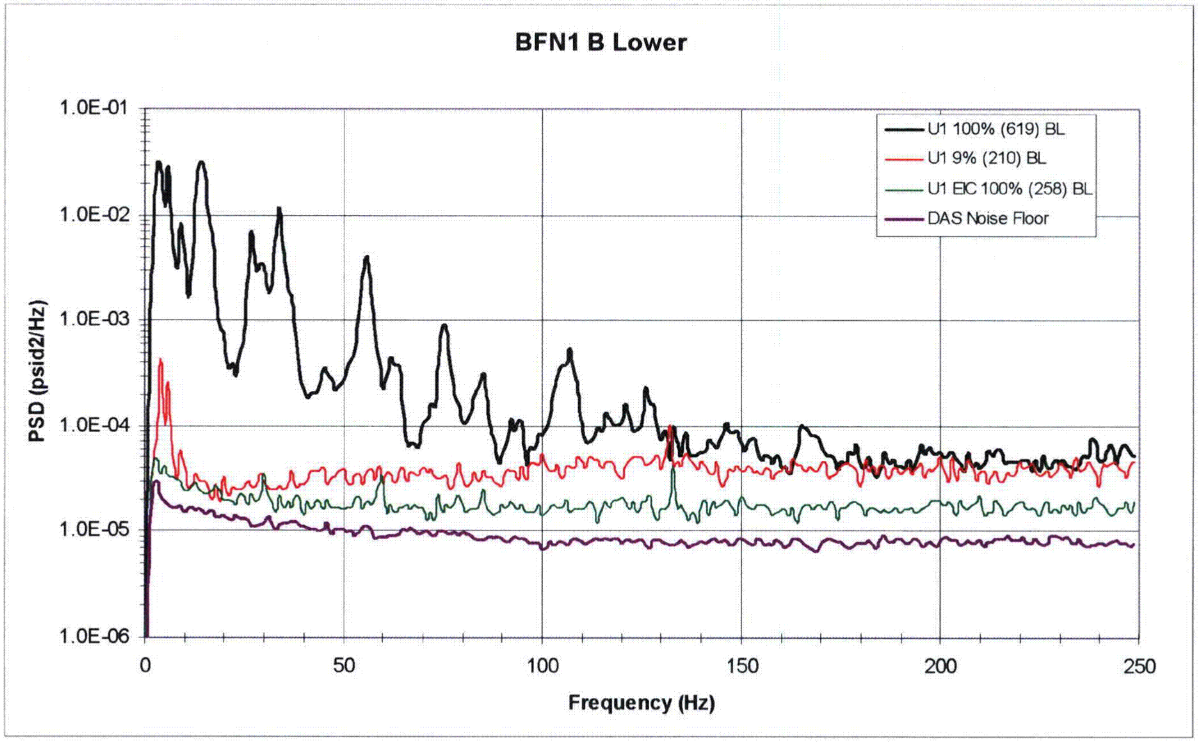

Figure EMCB.181-1b: Unit 1 Data MSL B

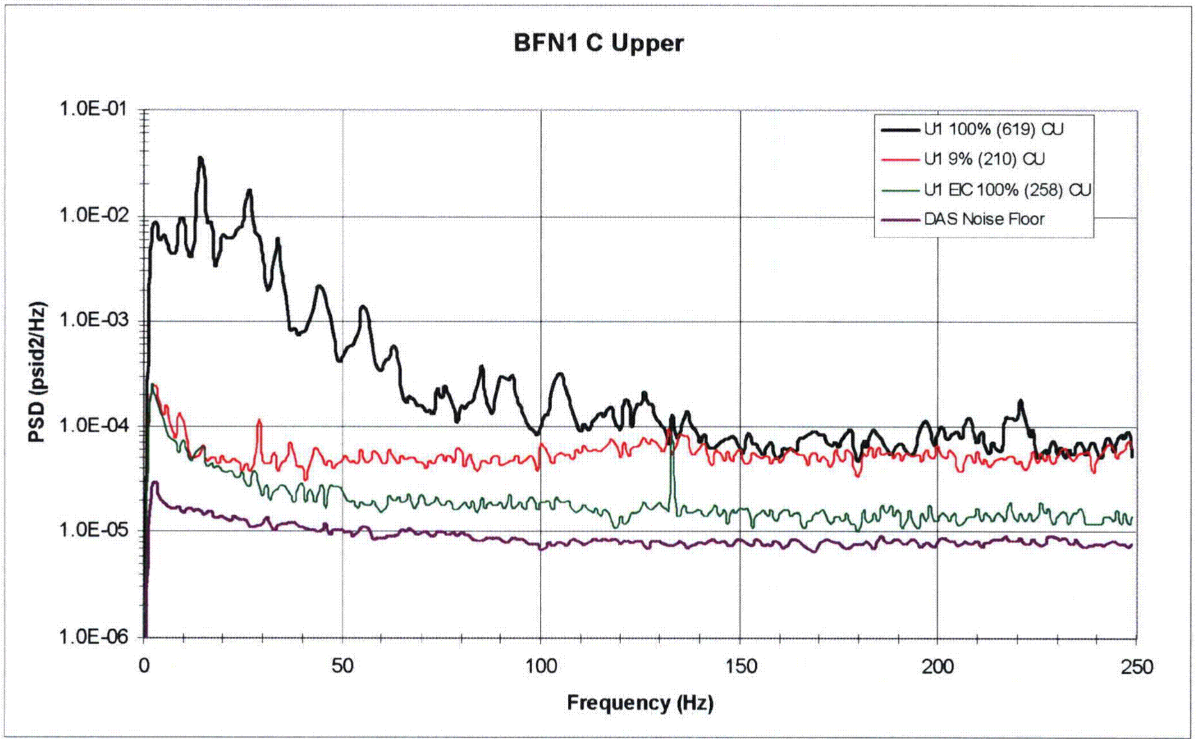

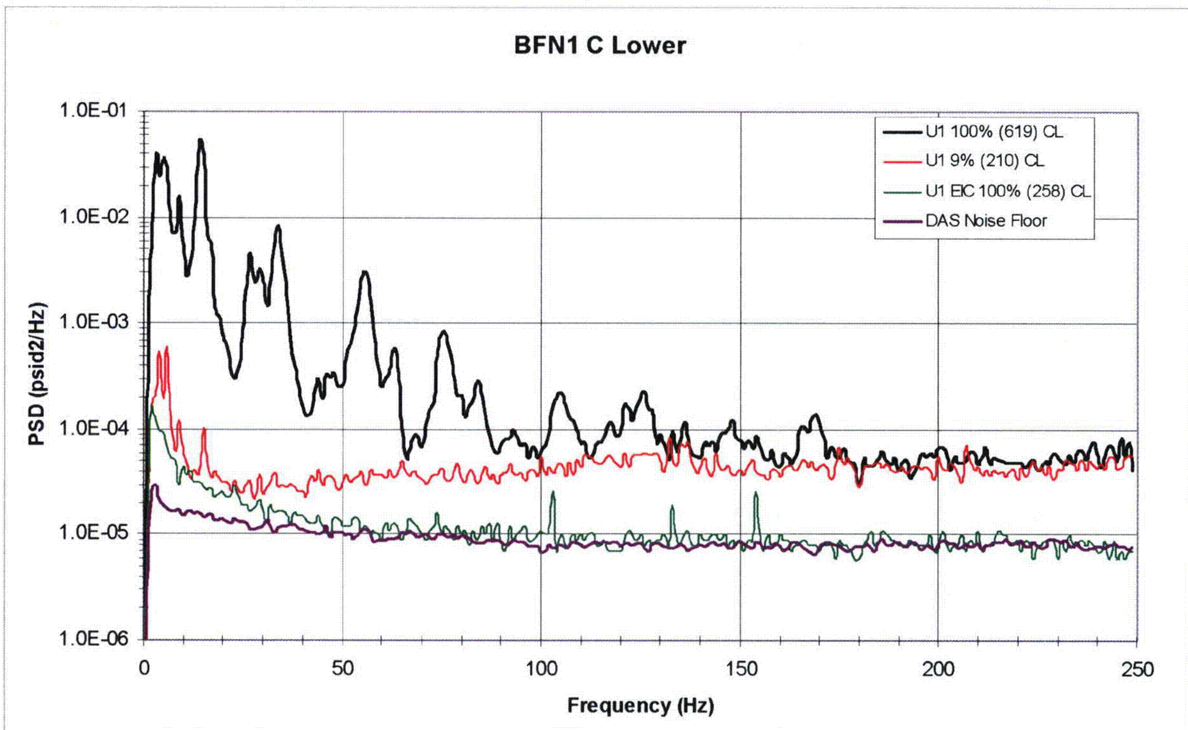

Figure EMCB.181-1c: Unit 1 Data MSL C

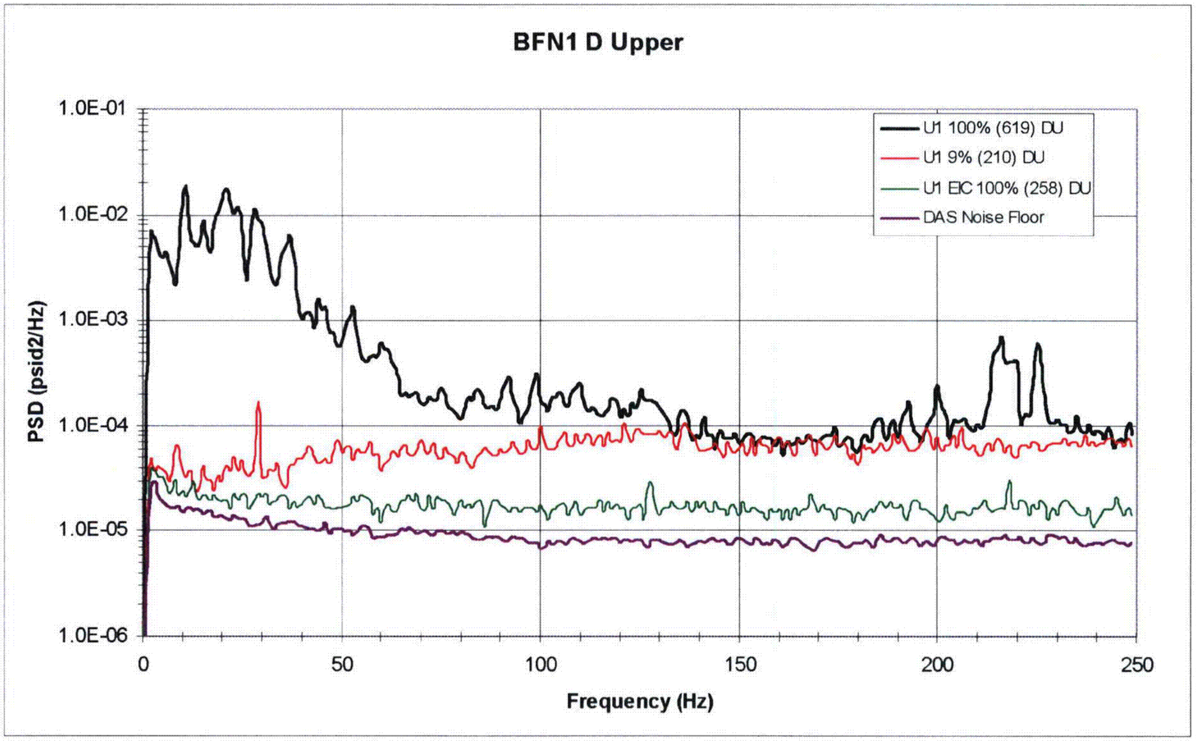

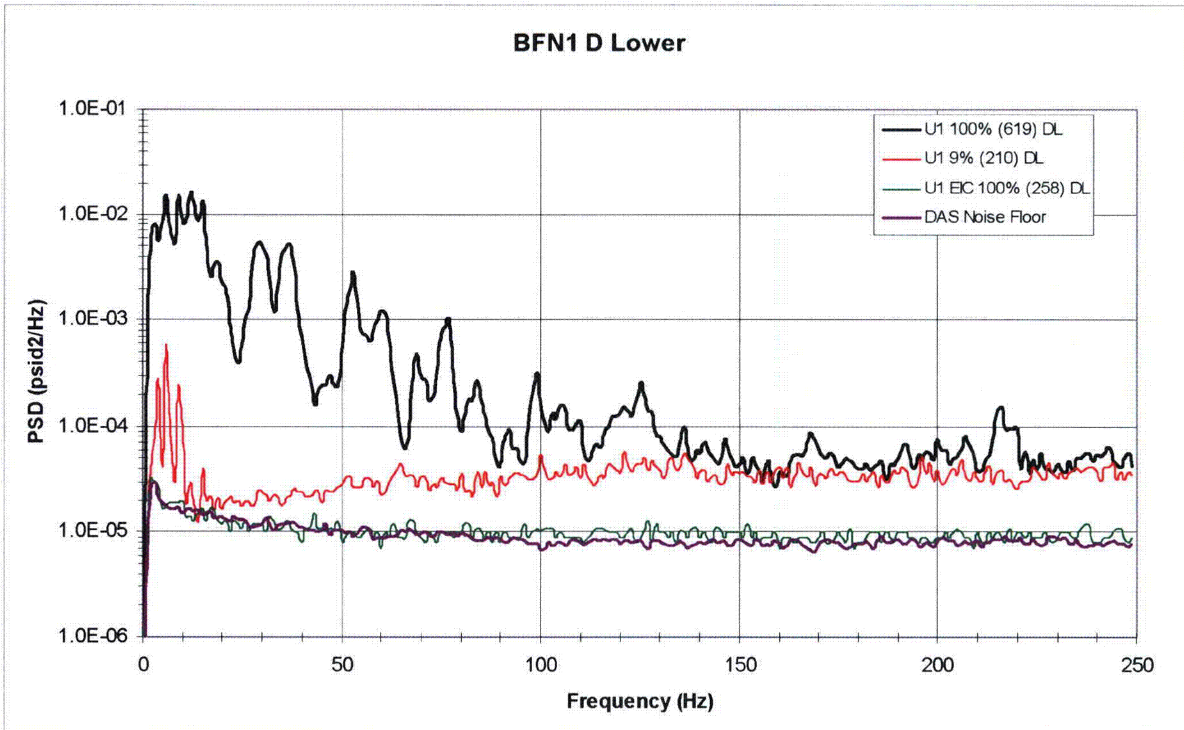

Figure EMCB.181-1d: Unit 1 Data MSL D

NRC RAI EMCB.182 (Unit 1 only)

The PSD comparisons of pressure measurements presented in the response to request for additional information (RAI) EMCB 172 (Figures EMCB 172-1 to 172-4) appear to contradict the comparisons presented in Continuum Dynamics Incorporated (CDI) Report 08-04P, *Acoustic and Low Frequency Hydrodynamic Loads at CLTP Power Level on Browns Ferry Nuclear Unit 1 Steam Dryer to 250 hertz (Hz)* (Figures 3.2-3.5). At frequencies above ~120 Hz, the response shows that the noise signals are lower than the corresponding signals at CLTP. However, CDI Report 08-04P shows the opposite. Explain why the information provided appears to be inconsistent. If the explanation for the inconsistency is that TVA chose a different plant MSL time history for the Unit 1 analysis, justify the change in time history

TVA Response to EMCB.182 (Unit 1 only)

The CLTP MSL strain gage data set reflected in Figures EMCB.172-1 through 4 is different from the CLTP MSL strain gage data set reflected in CDI Report 08-04P Figures 3.2 through 3.5 (see the response to RAI EMCB.180 in the June 16, 2008 submittal, "Response to Round 15 Group 4 and Round 17 Requests for Additional Information) (ML081750080). The CLTP data set was changed because it contained three atypical data spikes near the middle of the 120 seconds of data examined, specifically between 62.45 and 62.46 seconds, with peak pressures of 0.85 psid. All other peak pressures in the 120 second data set are below 0.6 psid, with an average peak pressure below 0.2 psid. Two other 120 second data sets were collected at CLTP power and neither of these displayed the data spike. It was concluded that the data spike was an anomaly that could not be reproduced, and one of the other two data sets was used in the subsequent analysis.

The CLTP plots in the response to RAI EMCB.172 and CDI Report 08-04P also differ in that the CLTP plots in CDI Report 08-04P show the result after EIC was subtracted. The CLTP plots in the response to RAI EMCB.172 do not have EIC subtracted.

The 9% power plots in the response to RAI EMCB.172 and CDI Report 08-04P are the same and do not include EIC subtraction. Since EIC was subtracted from the CLTP signal and not the 9% power signal in CDI Report 08-04P Figures 3.2 through 3.5, the CLTP plot is lower than the 9% power plots at frequencies above ~120 Hz. The relationship between CLTP and 9% power with no EIC subtraction is provided in Figures EMCB.181-1a through 1d and show that the CLTP signal is above the 9% power signal.

In the current methodology for noise removal (discussed in "Background" above), EIC is subtracted from both the CLTP signal and the LF signal prior to subtracting the LF signal from the CLTP signal. While CDI Report 08-04P Figures 3.2 through 3.5 only show EIC subtraction from the CLTP signal, CDI is in the process of verifying that the stress analysis results included EIC subtraction from both the CLTP and 9% power data.

NRC RAI EMCB.183 (Unit 1 only)

The accumulated stress plots presented in response to RAI EMCB 170/138 show that the alternating stress amplitude increases little beyond 100 Hz. Please explain this observation. Provide similar stress plots when unfiltered MSL signals are used for the stress analysis of Unit 1 dryer. Please explain the differences between the plots for filtered and unfiltered signals.

TVA Response to EMCB.183 (Unit 1 only)

The response to RAI EMCB 170/138 is based upon the analysis presented in CDI Report No. 08-06P which was provided in the submittal dated March 6, 2008, "Response to Round 15 RAI Regarding Steam Dryer Analyses, Group 2." The noise subtraction algorithm used to develop the accumulative PSDs for that response was the same as in CDI Report No. 08-06P and allowed the signal amplitude to be reduced down to zero if the noise amplitude exceeded the signal amplitude. The current noise reduction algorithm, and the one used for the most recent stress reports for both Unit 1 and 2 (CDI Reports No. 08-15P and 08-16P provided in the submittal dated June 16, 2008), allows no more than a 50% reduction of the CLTP signal amplitude. Table EMCB.183-1 compares the stress ratios obtained at the same locations examined in the response to RAI EMCB 170/138 using: (i) the original noise removal algorithm (allows all of the signal to be removed) used for the response to RAI EMCB 170/138; (ii) the noise removal algorithm used for CDI Reports No. 08-15P and 08-16P (allows up to 50% of the CLTP signal to be removed) and (iii) no noise removal.

Figures EMCB.183-1a through j shows the accumulative stress intensities without noise removal. To facilitate comparison, the accumulative alternating stress intensities presented in the response to RAI EMCB 170/138 using noise removal algorithm (i) above are also shown. As before, the accumulative alternating stress intensity, $\Sigma_a(f)$, is defined as the alternating stress computed when zeroing all stress harmonics for frequencies above f. It is computed in 5 Hz increments as explained in the response to RAI EMCB 170/138.

In all cases, with or without noise removal, the dominant increases in the accumulative alternating stress intensity occur below 100 Hz. With noise left in, node 104539 exhibits the strongest increase above 100 Hz, though still less than the rise below 100 Hz. At the worst case frequency shift (+10%) for this case, the increase in alternating stress intensity between 0 to 100 Hz is 3560 psi. The remaining increase above 100 Hz is 604 psi, or less than 17% of the 0-100 Hz rise. The other node with a significant increase above 100 Hz is node 102407 which shows a jump at approximately 120 Hz. The total increase for this node (noise left in and the worst case frequency shift of +2.5%) above 100 Hz is 703 psi which is 14% of the 0-100 Hz stress rise (4955 psi).

The relatively low increase in accumulative alternating stress intensities above 100 Hz implies that acoustic loads are lower at these frequencies and/or acoustic modes above 100 Hz do not excite significant structural modes. The latter would result from either mismatches between the acoustic and structural mode frequencies or low coupling between the acoustic and structural mode shapes, or both. With minor exceptions (e.g., node 102,521) $\Sigma_a(f)$ increases above 100 Hz by approximately comparable amounts both with and without frequency shift. This suggests that there is no pronounced acoustic mode that is strongly coupled to a structural mode in this range. Strongly coupled modes do exist (for example, these gave rise to a strong 218 Hz structural response observed in Figures 19 and 20 of CDI Report No. 07-05P provided in the July 27, 2007 submittal, "Steam Dryer Evaluations," ML072130371). However, these do not have a strong signal.

The differences between the filtered and unfiltered stress responses can mostly be attributed to higher rises (with noise left in) in the 35-65 Hz range. This is consistent with the fact that the noise removal algorithm reduced the signal amplitude where the noise is high. These reductions are quantified in the response to RAI EMCB 170/138.

Finally, it is re-emphasized that the differences between the stress intensities with and without noise removal are smaller than the ones shown here when the later noise removal algorithm is used that limits signal amplitude reductions to 50% or less.

Table EMCB.183-1. List of nodes on welds in the BFN Unit 1 dryer having the lowest alternating stress ratios.

Location	Node	Freq. Shift (%)	Up to 100% amp. red.		Up to 50% amp. red.		No filtering	
			SR-P	SR-a	SR-P	SR-a	SR-P	SR-a
1. Top Cover Inner Hood/Top Cover Overlap/Top Perf. Plate	88059	+5	3.03	1.56	3.25	1.57	2.87	1.38
2. Top Cover/Tie Bar Base	107054	+10	3.47	1.59	3.39	1.64	2.96	1.43
3. Top Cover/Tie Bar Base	102407	+2.5	3.29	1.62	3.37	1.60	2.59	1.21
4. Top Cover Middle Hood/Top Perf. Plate/Top Cover Overlap	91420	+10	3.05	1.63	3.58	1.65	2.94	1.35
5. Top Cover/Tie Bar Base	96561	+10	3.96	1.94	4.00	1.94	3.47	1.68
6. Top Perf/Top Cover/Dam Plate	103088	+7.5	4.31	1.98	4.31	1.96	3.64	1.67
7. Submerged Drain Channel/Skirt	104539	+10	2.57	2.15	4.66	2.14	3.53	1.65
8. Dam Plate/Lock	102521	+7.5	4.76	2.19	4.50	2.10	3.64	1.71
9. Top Cover Inner Hood/Hood Support/Tie Bar Base	103094	+10	4.00	2.28	4.37	2.23	3.65	1.90
10. Top Perf/Top Cover/Dam Plate	103089	+5	5.14	2.4	5.17	2.37	4.23	1.97

Node 88059

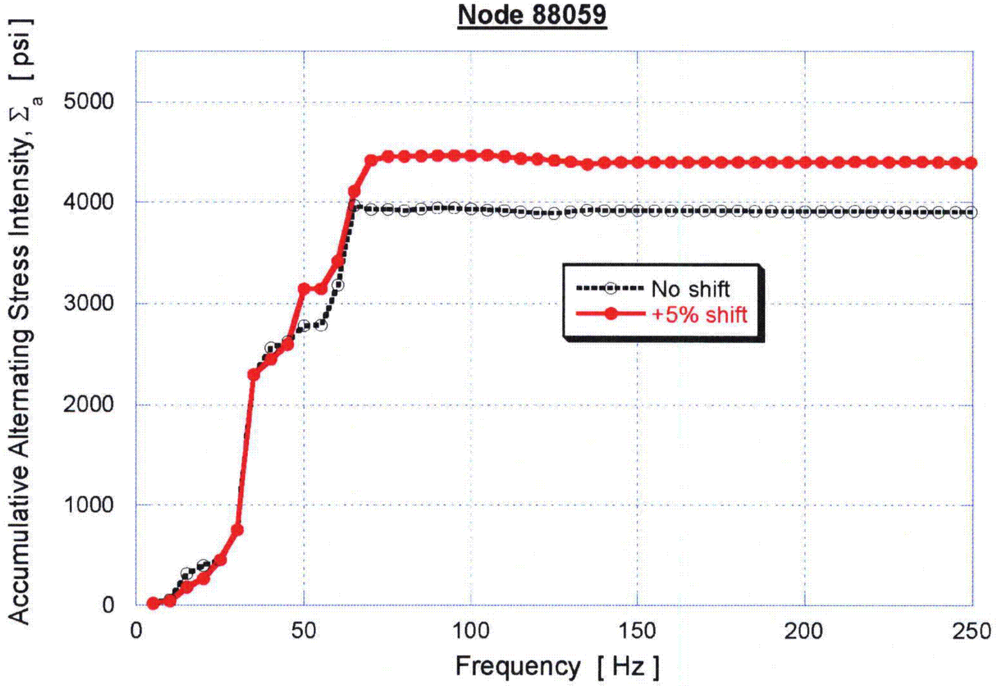

Full noise removal

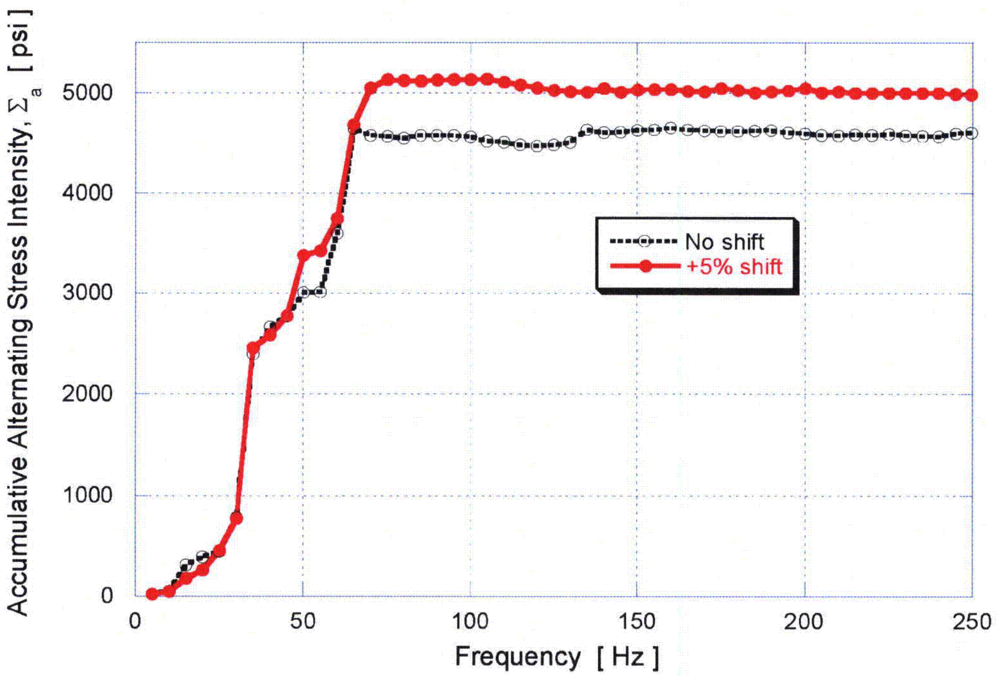

No noise removal

Figure EMCB.183-1a: Accumulative alternating stress intensity curves for node 88059

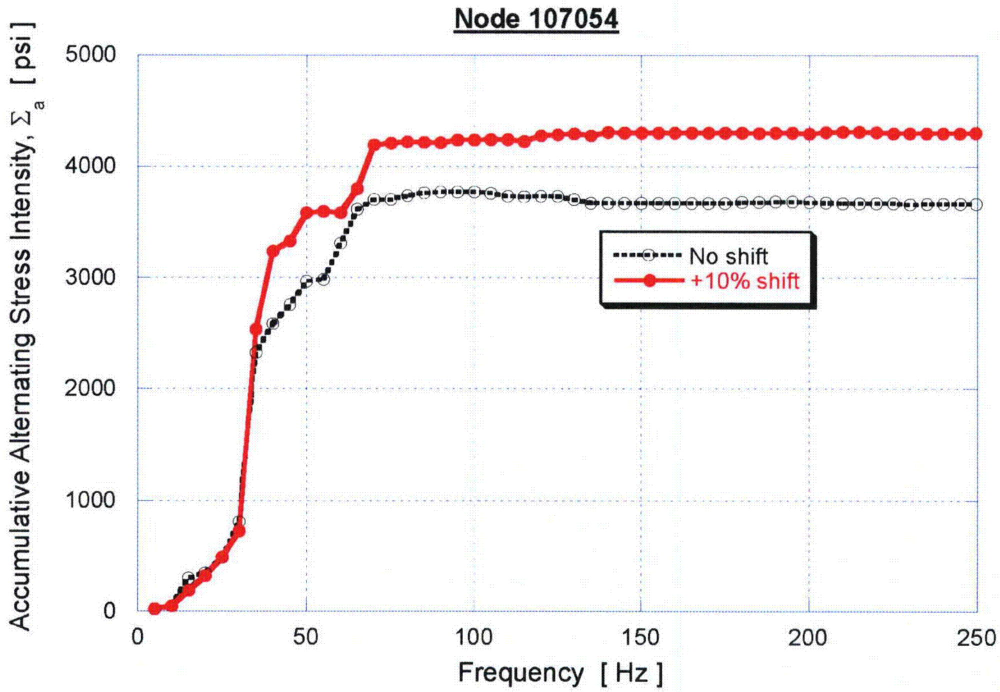

Full noise removal

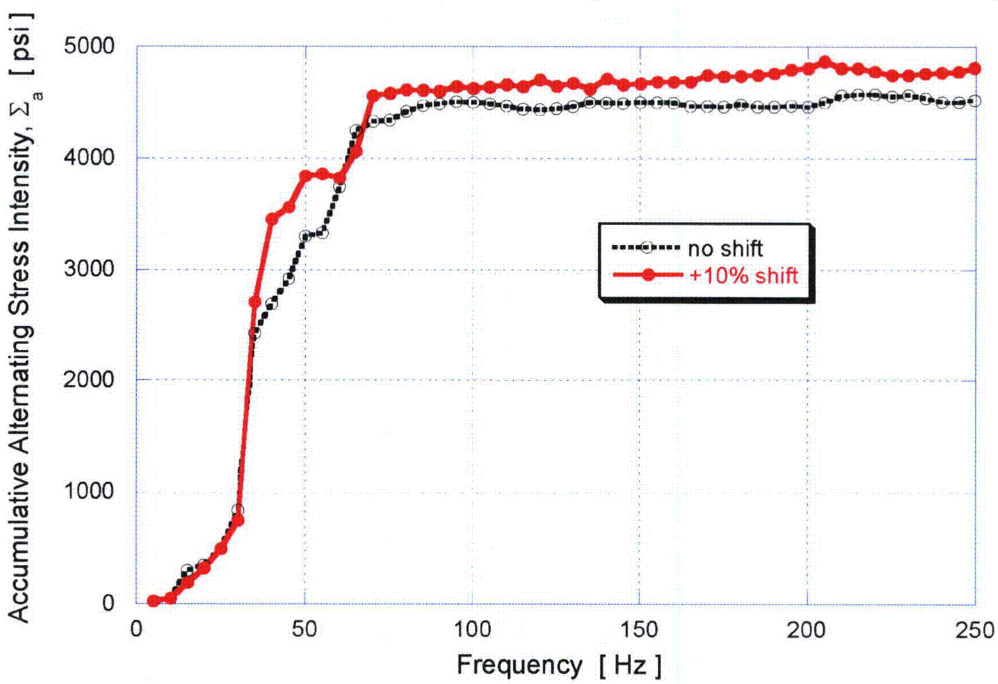

No noise removal

Figure EMCB.183-1b: Accumulative alternating stress intensity curves for node 107054

Node 102407

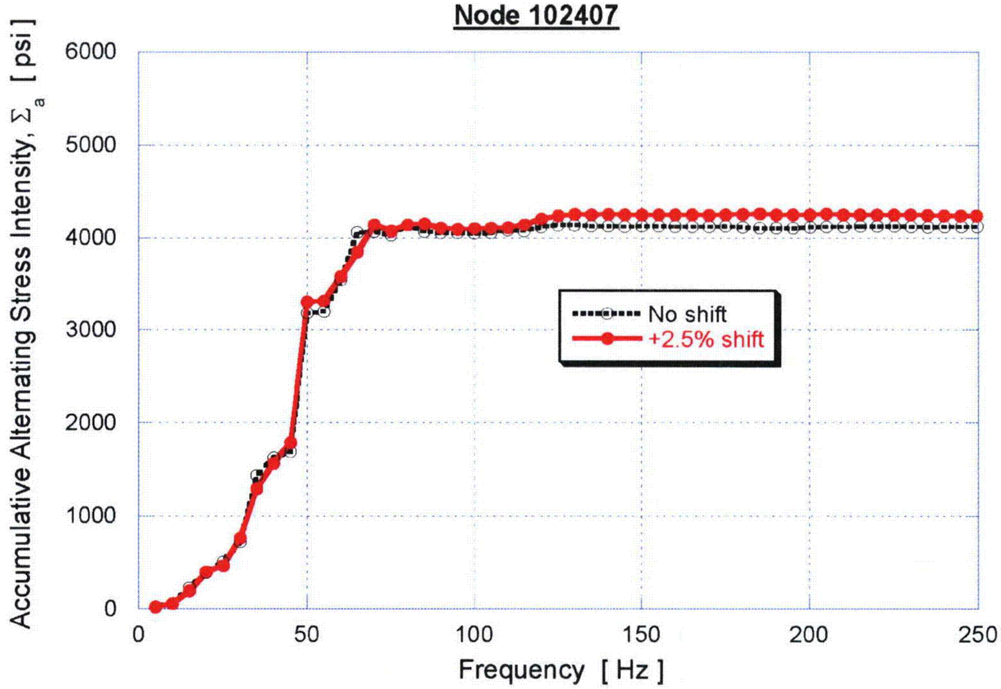

Full noise removal

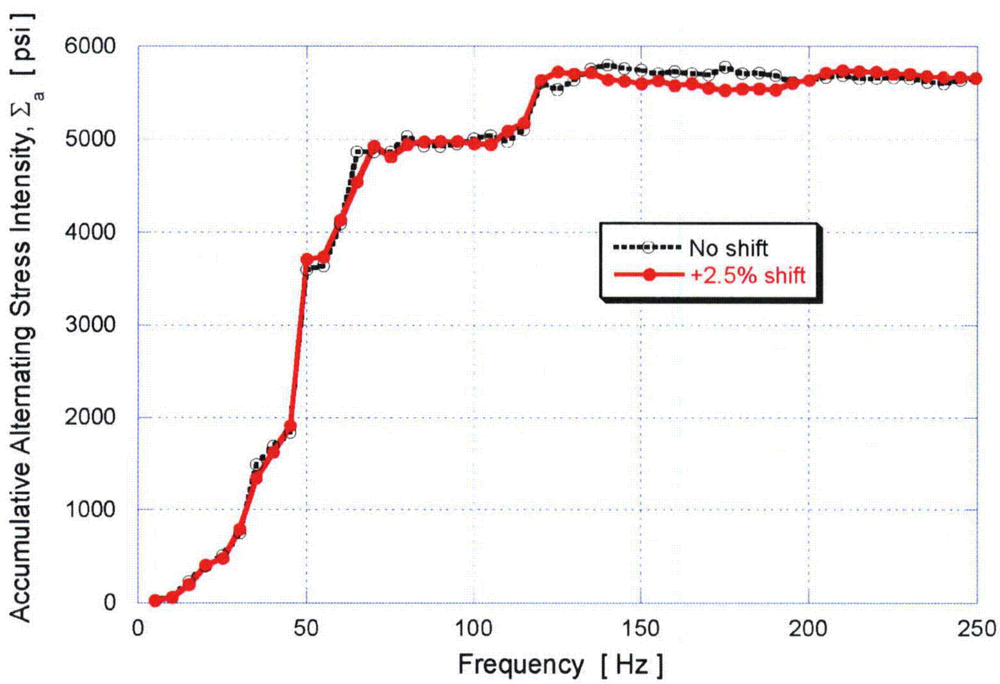

No noise removal

Figure EMCB.183-1c: Accumulative alternating stress intensity curves for node 102407

NON-PROPRIETARY INFORMATION

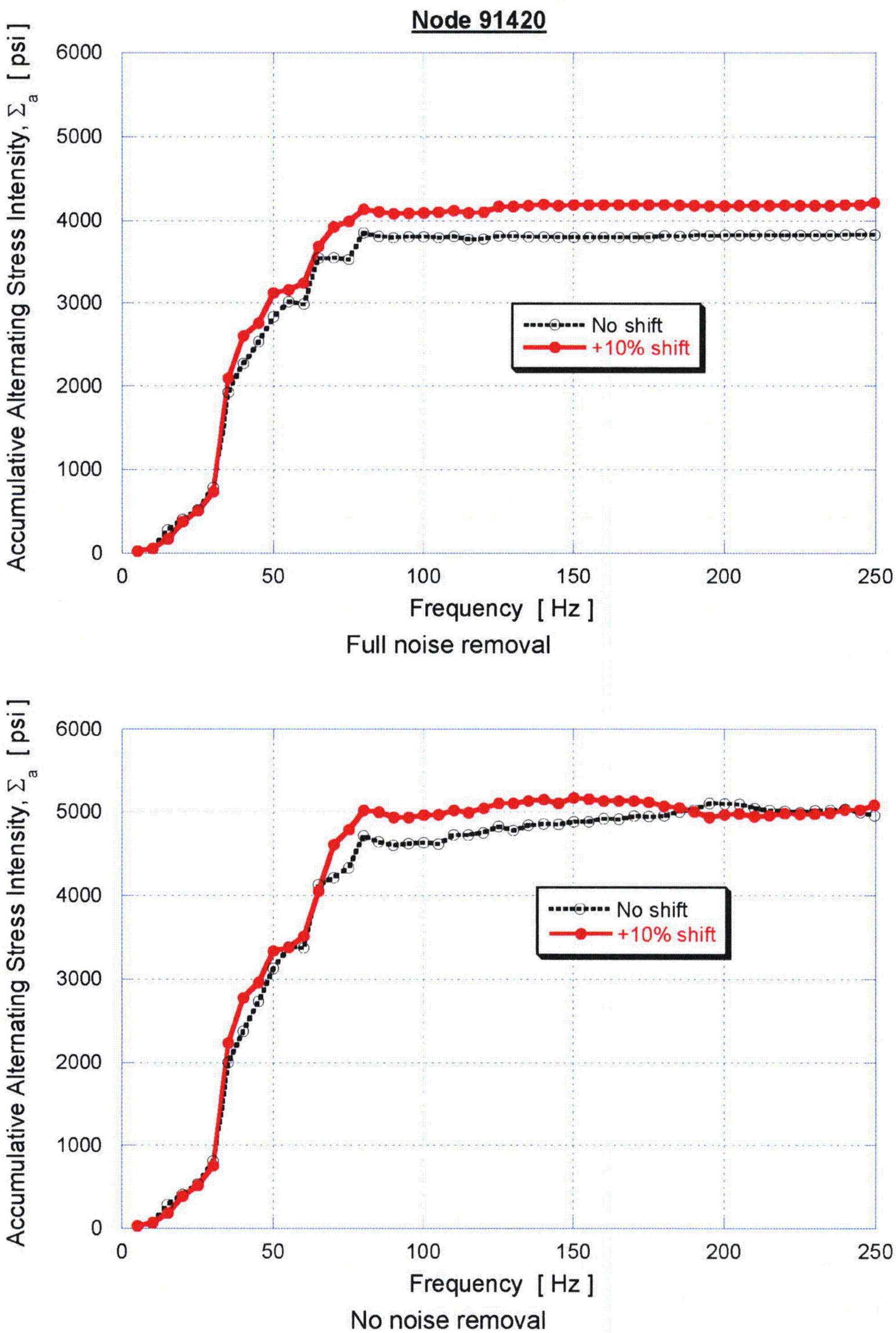

Figure EMCB.183-1d: Accumulative alternating stress intensity curves for node 91420

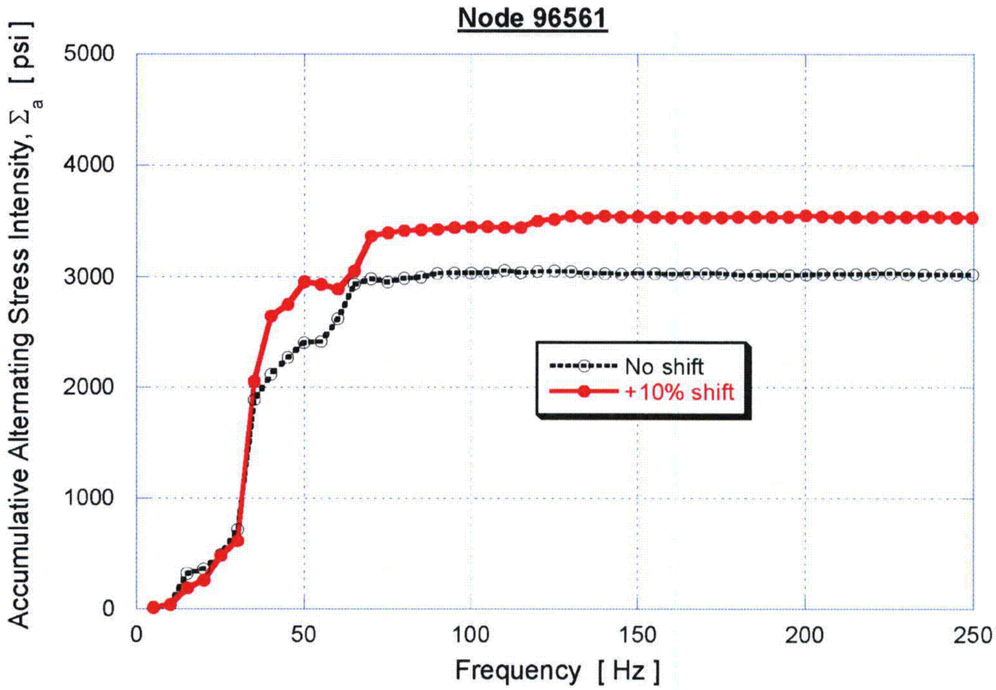

Full noise removal

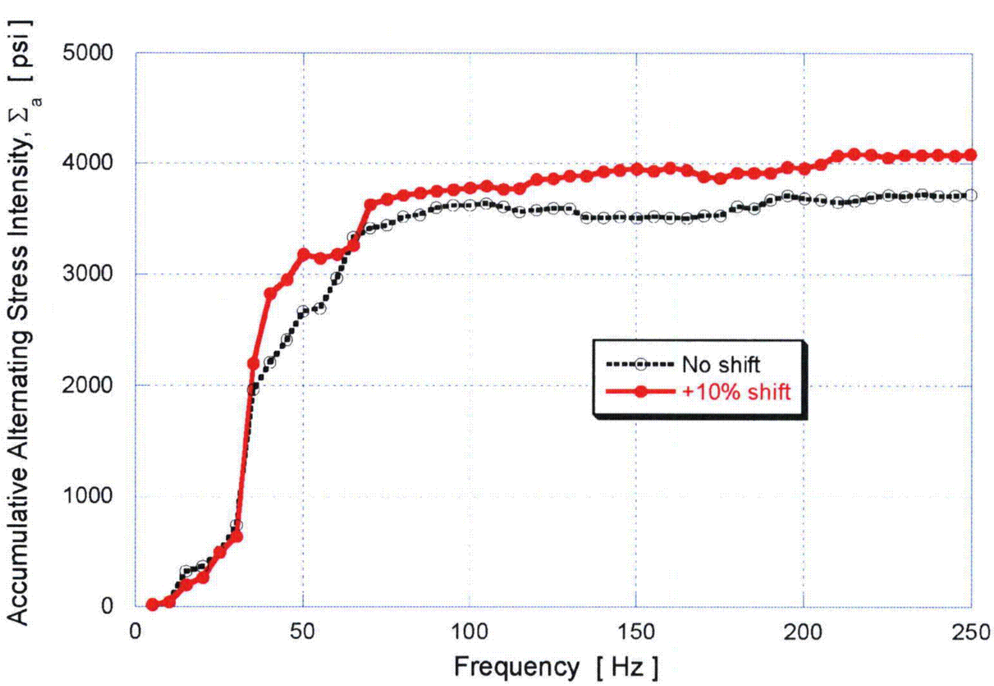

No noise removal

Figure EMCB.183-1e: Accumulative alternating stress intensity curves for node 96561

NON-PROPRIETARY INFORMATION

Node 103088

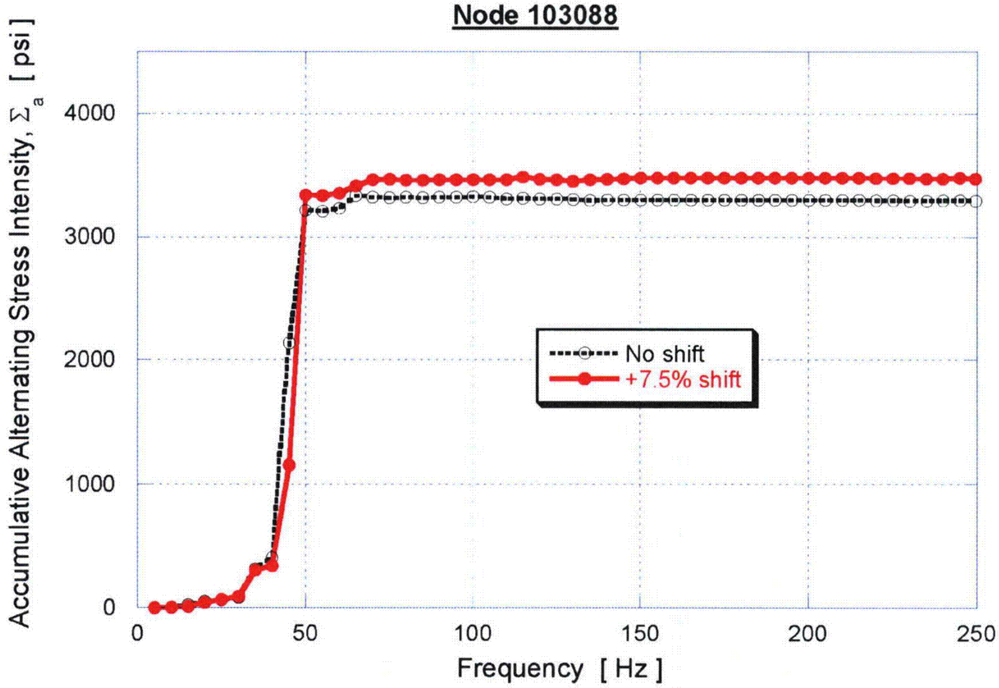

Full noise removal

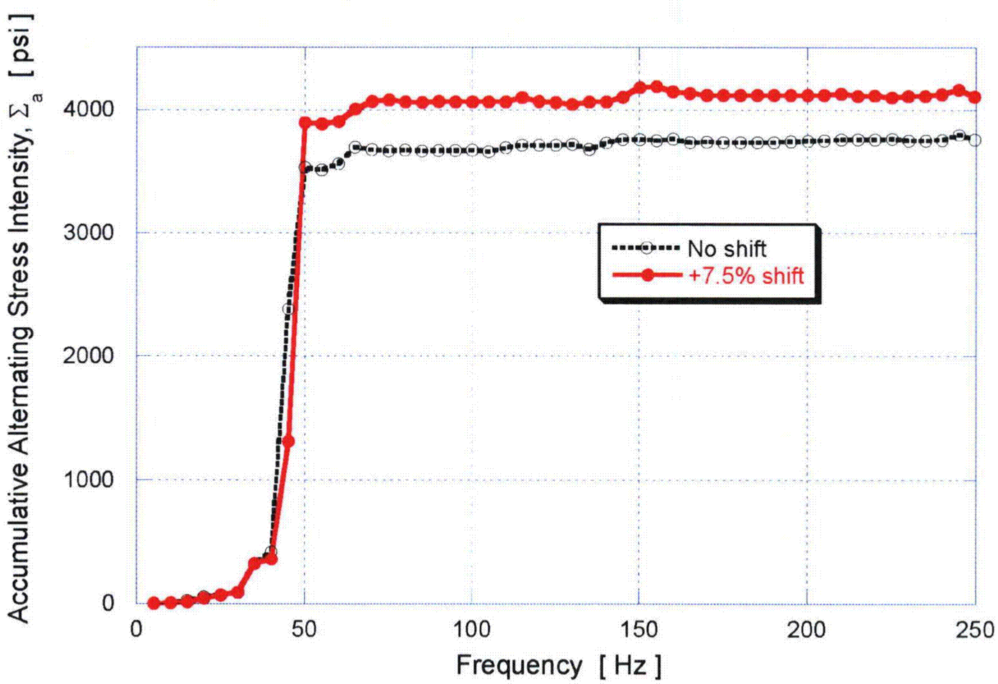

No noise removal

Figure EMCB.183-1f: Accumulative alternating stress intensity curves for node 103088

Node 104539

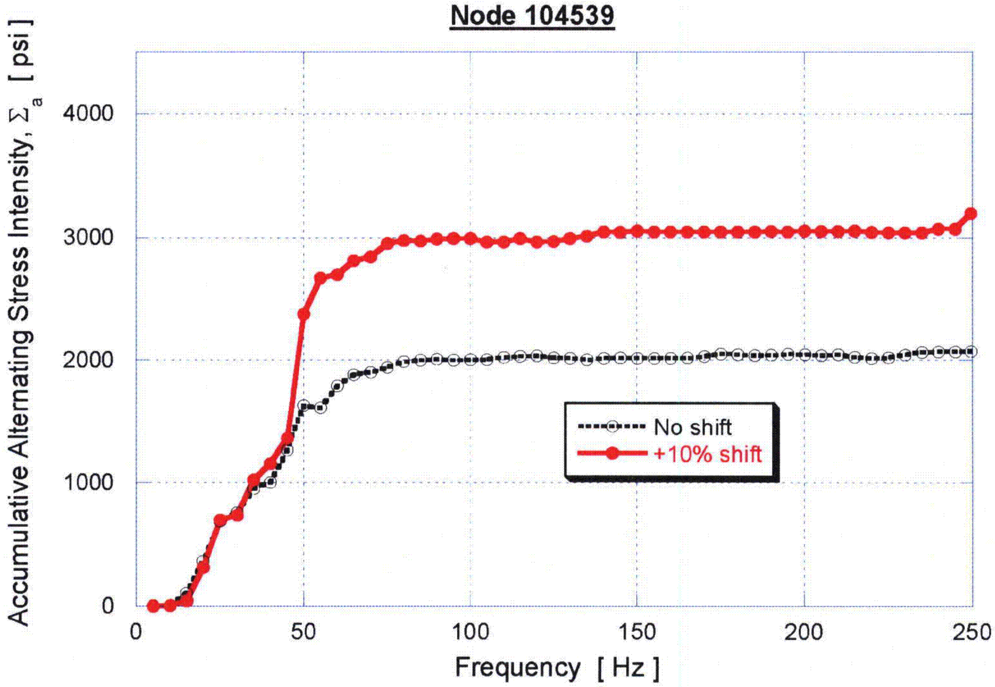

Full noise removal

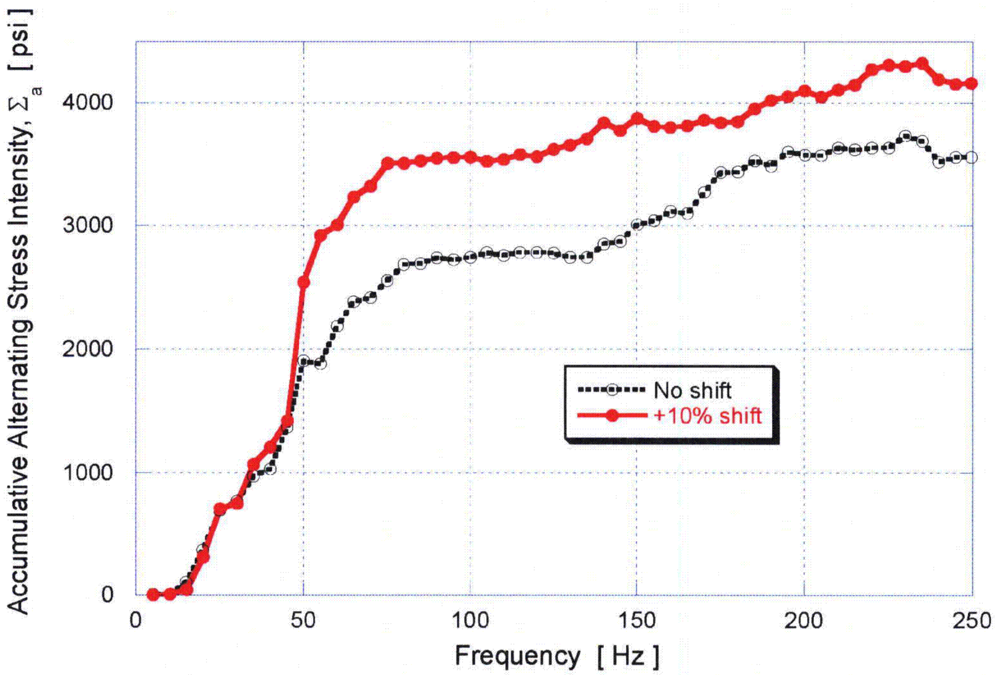

No noise removal

Figure EMCB.183-1g: Accumulative alternating stress intensity curves for node 104539

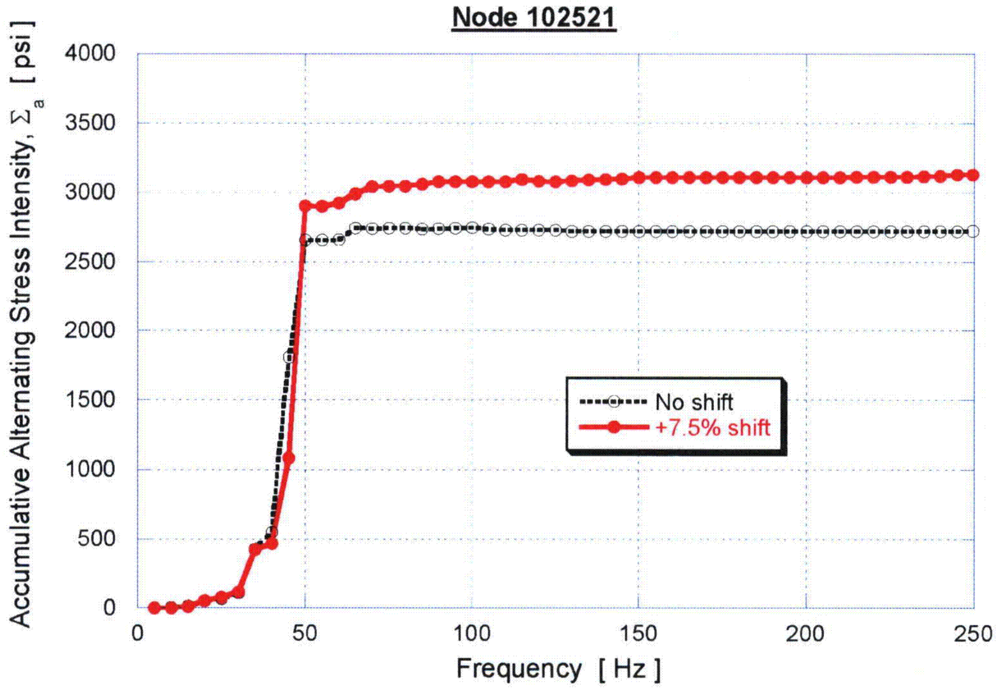

Full noise removal

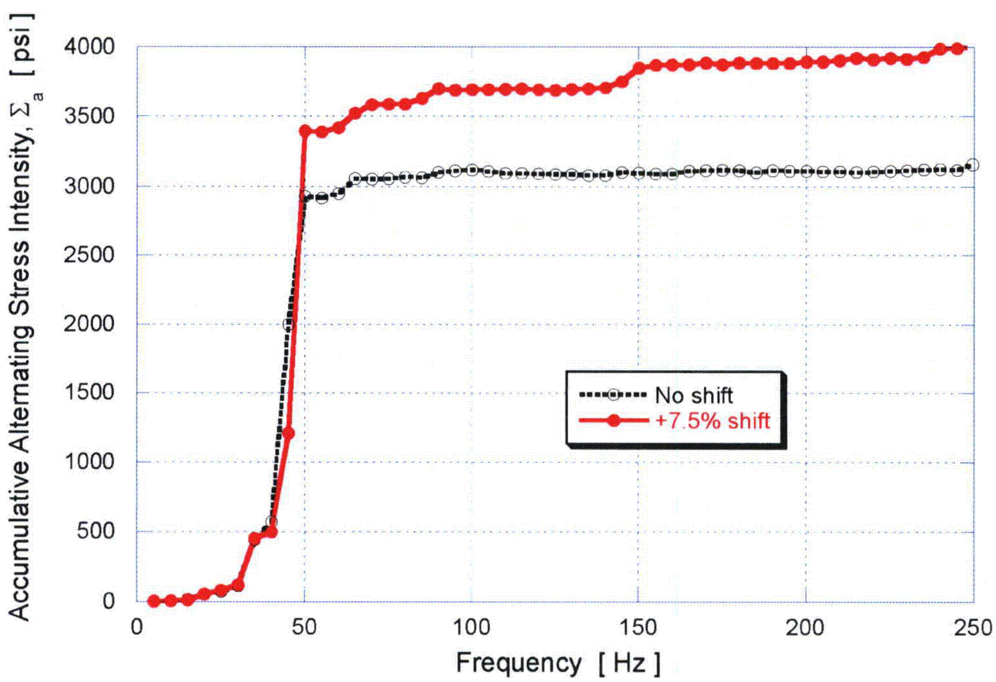

No noise removal

Figure EMCB.183-1h: Accumulative alternating stress intensity curves for node 102521

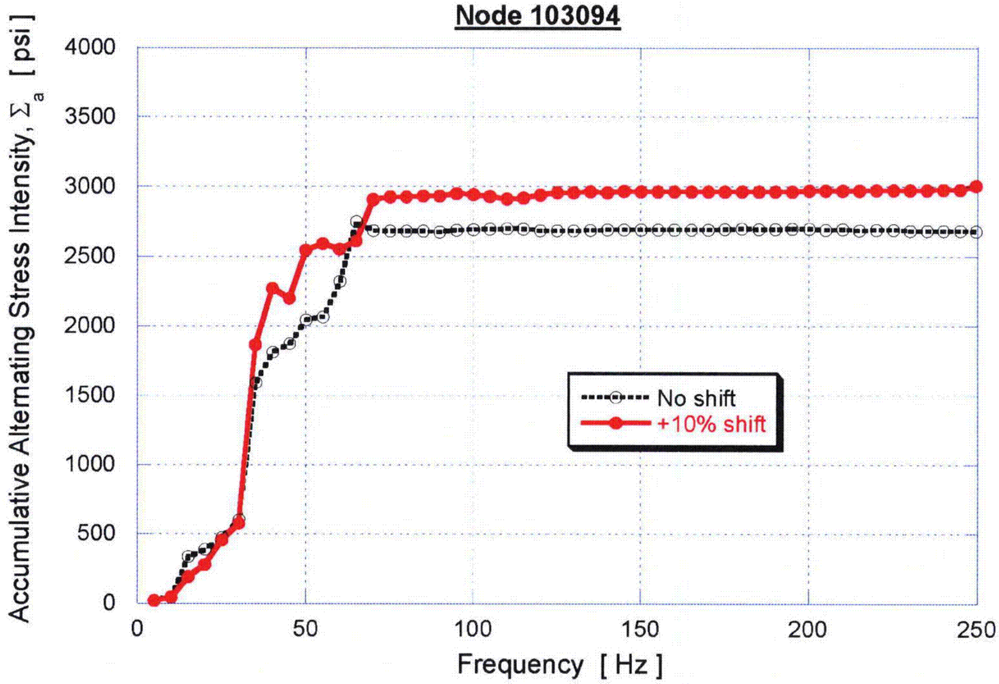

Full noise removal

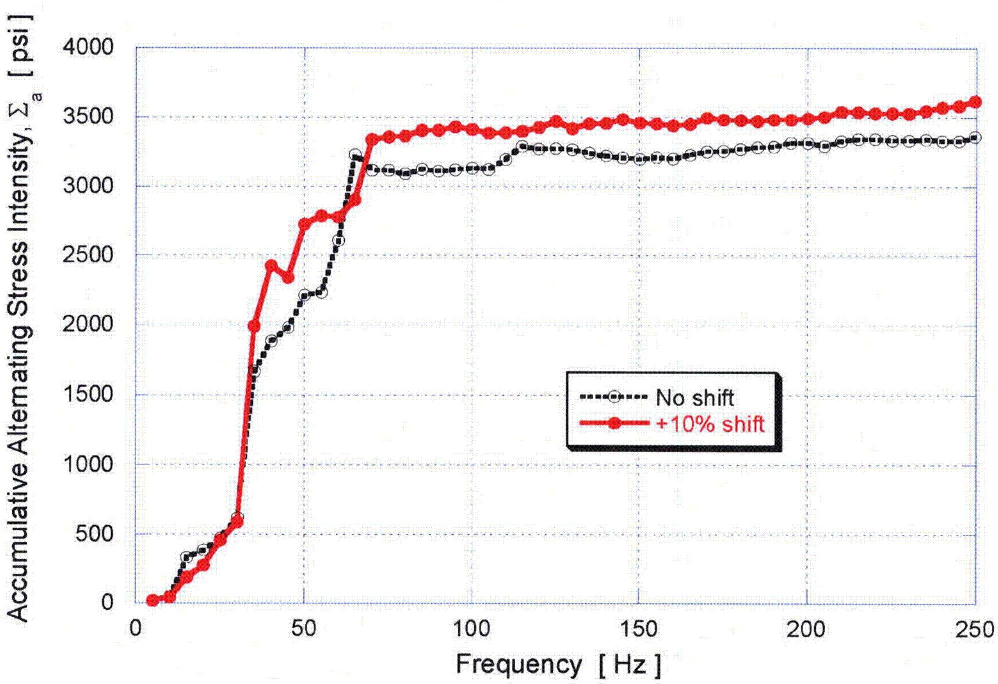

No noise removal

Figure EMCB.183-1i: Accumulative alternating stress intensity curves for node 103094

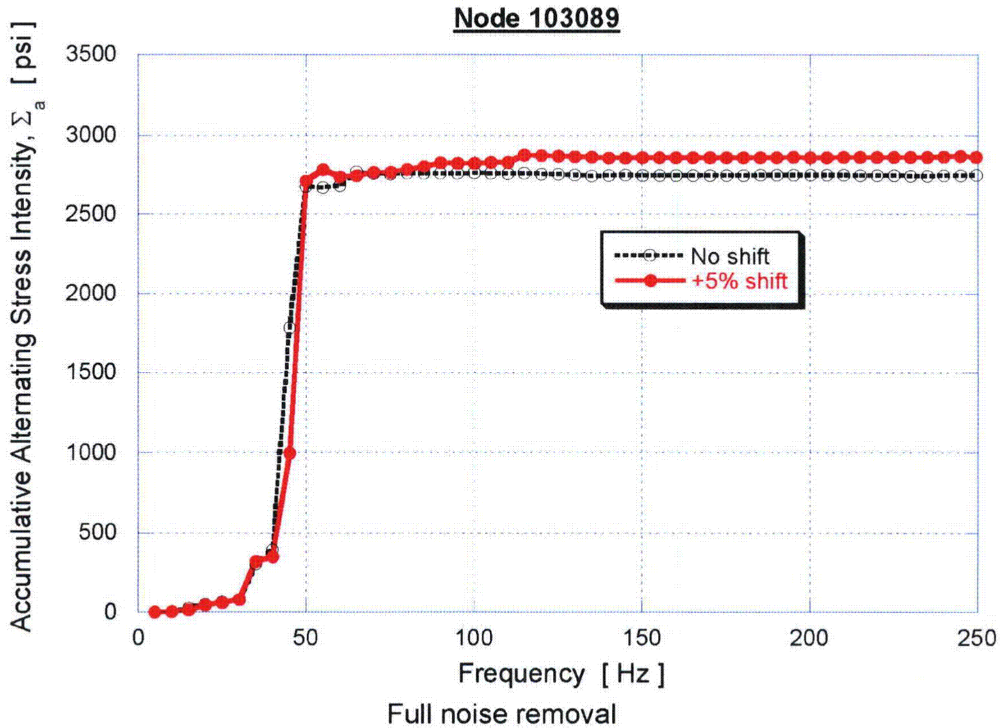

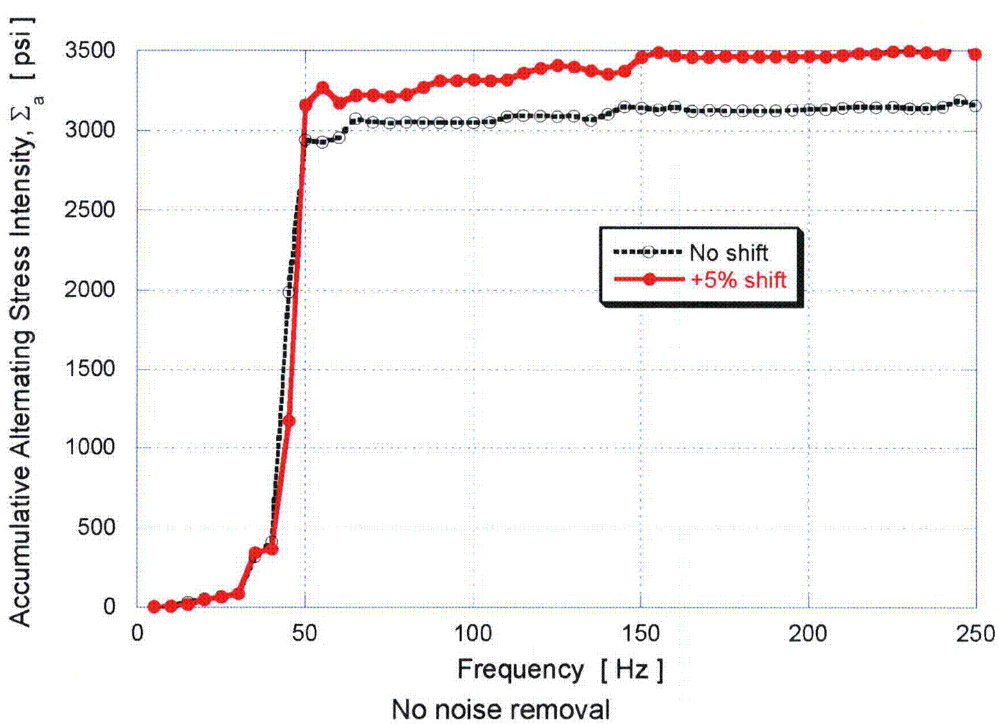

Figure EMCB.183-1j: Accumulative alternating stress intensity curves for node 103089

NRC RAI EMCB.147 (Unit 2 only)

Provide analysis and plots for Unit 2 similar to those provided for Unit 1 in response to RAI EMCB.172. Provide an explanation why the 19 percent power data shown in Figures 3.2 through 3.5 in CDI Report No. 08-05P, *Acoustic and Low Frequency Hydrodynamic Loads at CLTP Power Level on Browns Ferry Nuclear Unit 2 Steam Dryer to 250 Hz*, are higher than the data at CLTP for frequencies above about 120 Hz. Provide justification for removing any signal from the Unit 2 CLTP source strengths without reliable background noise signals. TVA should include stress and stress ratio tables in CDI Report 08-16P, *Stress Assessments of Browns Ferry Nuclear Unit 2 Steam Dryer with Tie Bar and Hood Modifications*, using unfiltered MSL signals.

TVA Response to EMCB.147 (Unit 2 only)

Figures EMCB.147-1a through 1d show PSD plots of available Unit 2 data including 19% power, 30% power, CLTP and an EIC signal taken at CLTP conditions. It can be seen from the EIC signal that Unit 2 data contains electrical noise that increases with frequency above 80 Hz. The most likely source of this noise is the VFD providing power to the 2A recirculation pump due to the close proximity of the strain gage signal penetrations to the pump power penetrations. The recirculation pumps are powered by VFDs which produce AC waveforms using multilevel pulse width modulation. Therefore, strong coupling of the signal may be expected to result in harmonic noise. By comparing the 19% power, 30% power and CLTP signals, it can also be seen that as power increases from 19% to 30%, the amplitude above 150 Hz decreases to that of the CLTP value. Analysis of Unit 1 data (see Figures EMCB.181-1a through 1d) shows that the amplitude of MSL strain gage data does not change significantly with steam flow and power level above 150 Hz. The most likely cause for the behavior of Unit 2 data is a decrease in the 150 - 250 Hz spectral content of noise contribution from the Unit 2 VFD as recirculation pump speed is increased from minimum speed (~16 Hz) at 19% power to ~ 25 Hz at 30% power.

Due to the unique noise characteristics of the Unit 2 data, the 30% power signal is more suitable for use as a LF signal at frequencies between 150 to 250 Hz. During a teleconference with the NRC on August 15, 2008, it was agreed that a composite LF signal would be developed by using the more limiting amplitude of the 19% power and 30% power signals at each frequency from 0 to 250 Hz. TVA is in the process of generating the composite LF signal to confirm that the Unit 2 stress analysis results remain acceptable using this signal. The results of this analysis will be provided by September 19, 2008.

Figures EMCB.147-1a through 1d are PSD plots of Unit 2 signals which illustrate example signal magnitudes. The signals were filtered at the following frequencies to eliminate known noise sources.

CLTP

Frequency Range (Hz)	Filtering
0 - 2	Mean
59.8 - 60.2	Line Noise
119.9 - 120.1	Line Noise
179.8 - 180.2	Line Noise
239.9 - 240.1	Line Noise
44 - 46 89.5 - 90.5 135.5 - 136.5 180.5 - 181.5 226.5 - 227.5	VFD
111-112	Recirc Pumps A, B Speed (5x)
217-220	Standpipe Excitation

19% Power

Frequency Range (Hz)	Filtering
0 - 2	Mean
59.8 - 60.2	Line Noise
119.9 - 120.1	Line Noise
179.8 - 180.2	Line Noise
239.9 - 240.1	Line Noise
15 - 16 31.5 - 32.5 47.5 - 48.5 63.5 - 64.5 79.5 - 80.5 95.5 - 96.5 111.5 - 112.5 127.5 - 128.5 143.5 - 144.5 159.5 - 160.5 175.5 - 176.5 191.5 - 192.5 207.5 - 208.5 223.5 - 224.5 239.5 - 240.5 255.5 - 256.5	VFD

NON-PROPRIETARY INFORMATION

30% Power

Frequency Range (Hz)	Filtering
0 - 2	Mean
59.8 - 60.2	Line Noise
119.9 - 120.1	Line Noise
179.8 - 180.2	Line Noise
239.9 - 240.1	Line Noise
23.5 - 24.5 48.5 - 49.5 72.5 - 73.5 97.5 - 98.5 122.5 - 123.5 146.5 - 147.5 171.5 - 172.5 196.5 - 197.5 220.5 - 221.5 245.5 - 246.5	VFD
60.5 - 61.5	Recirc Pumps A, B Speed (5x)

EIC

Frequency Range (Hz)	Filtering
0 - 2	Mean
59.8 - 60.2	Line Noise
119.9 - 120.1	Line Noise
179.8 - 180.2	Line Noise
239.9 - 240.1	Line Noise
44 - 46 89.5 - 90.5 135.5 - 136.5 180.5 - 181.5 226.5 - 227.5	VFD

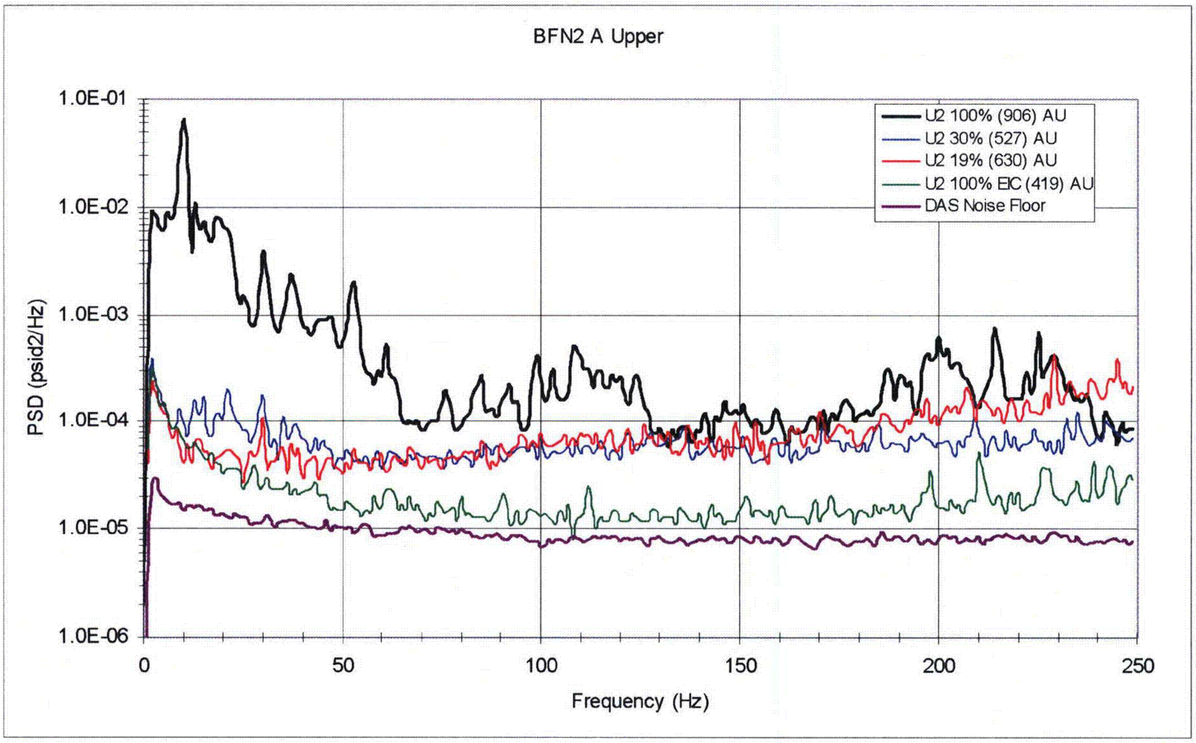

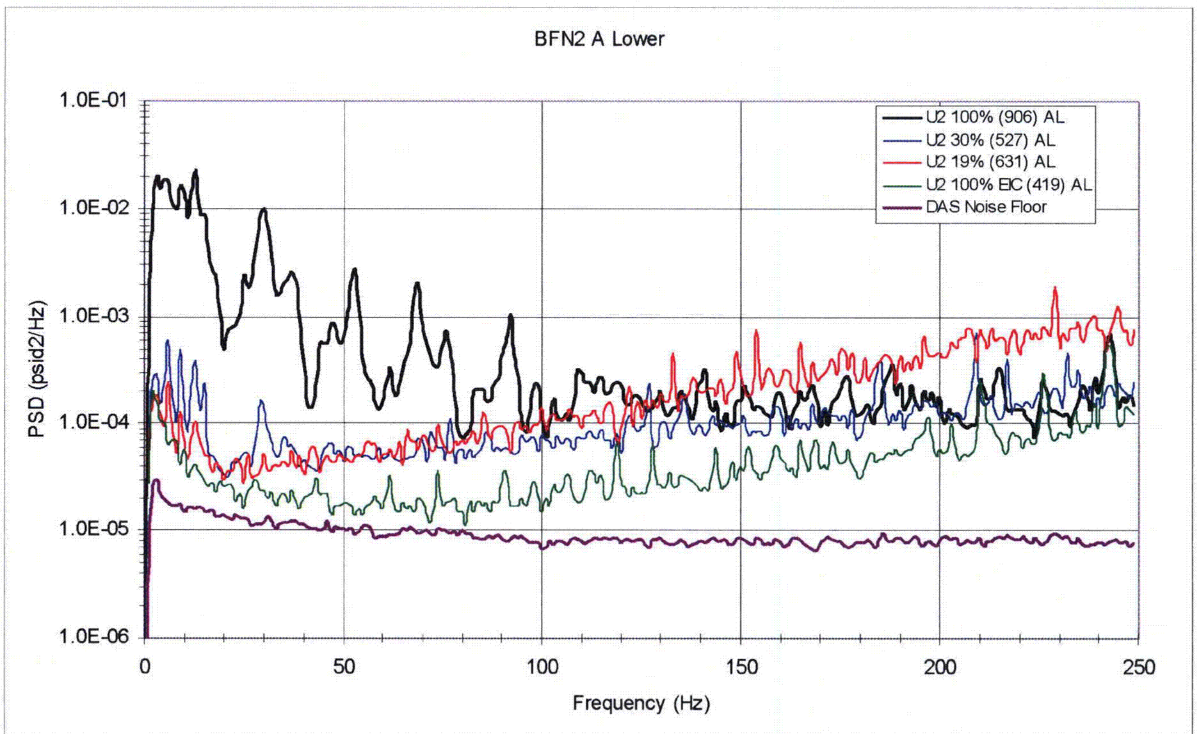

Figure EMCB.147-1a: Unit 2 Data MSL A

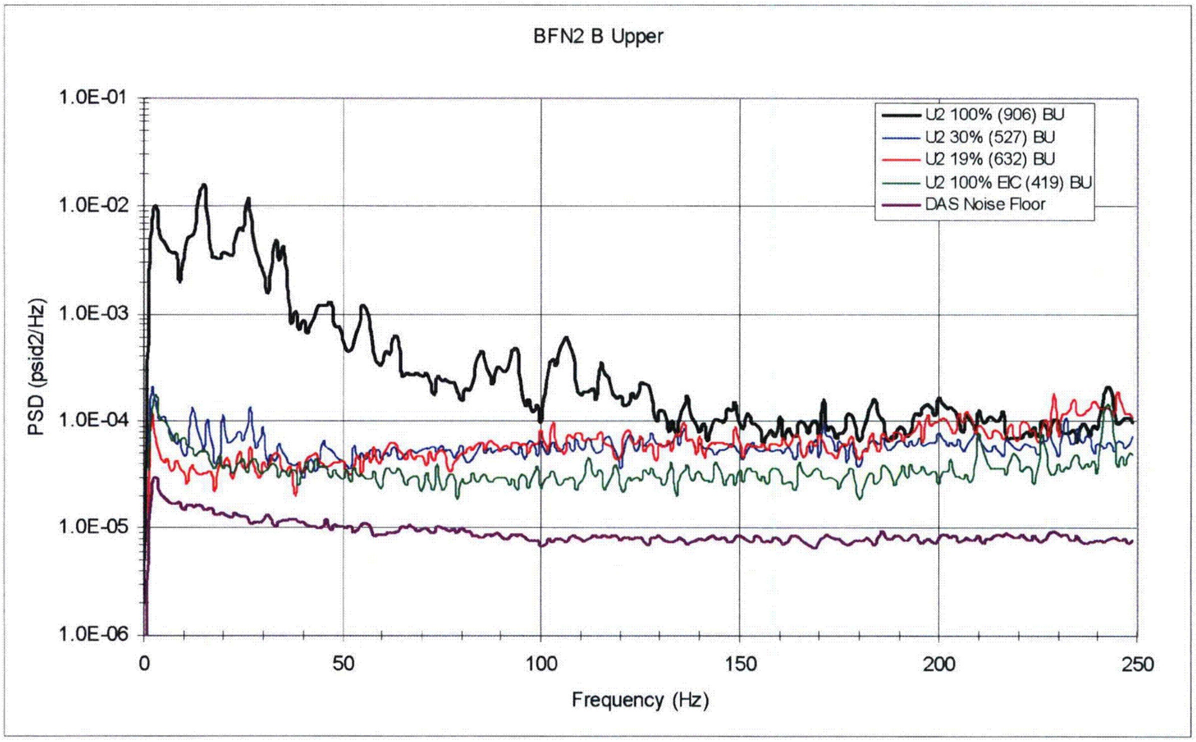

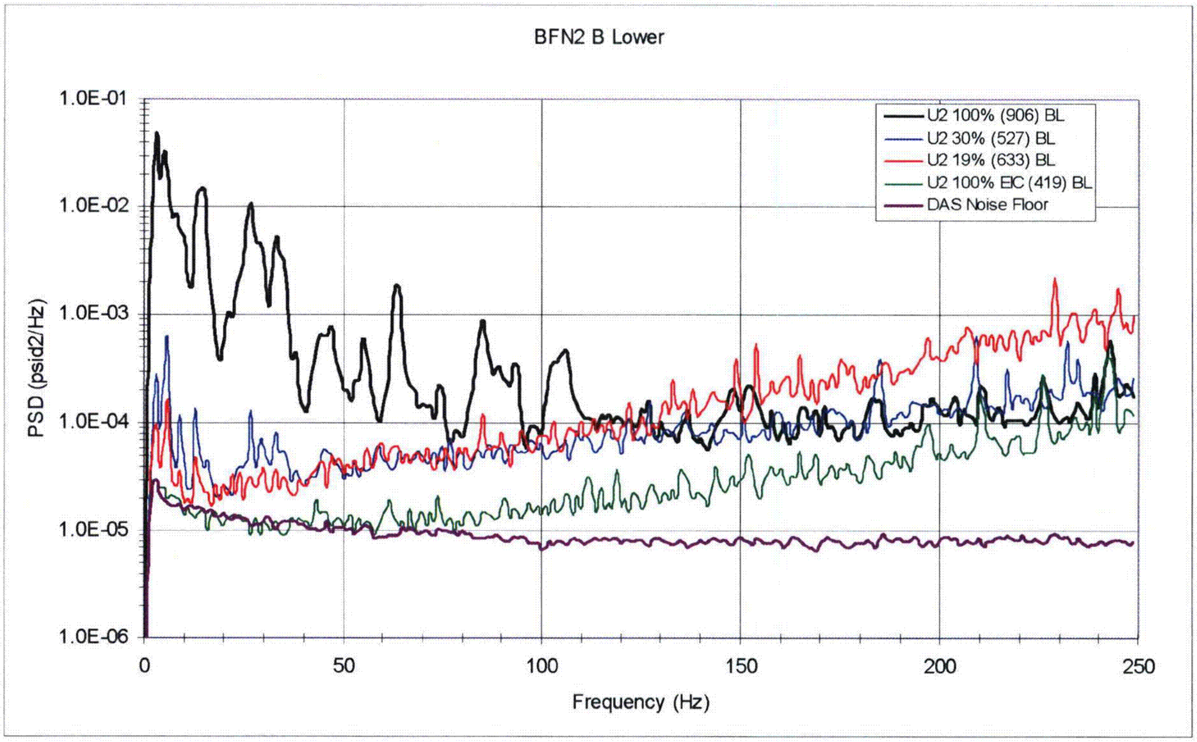

Figure EMCB.147-1b: Unit 2 Data MSL B

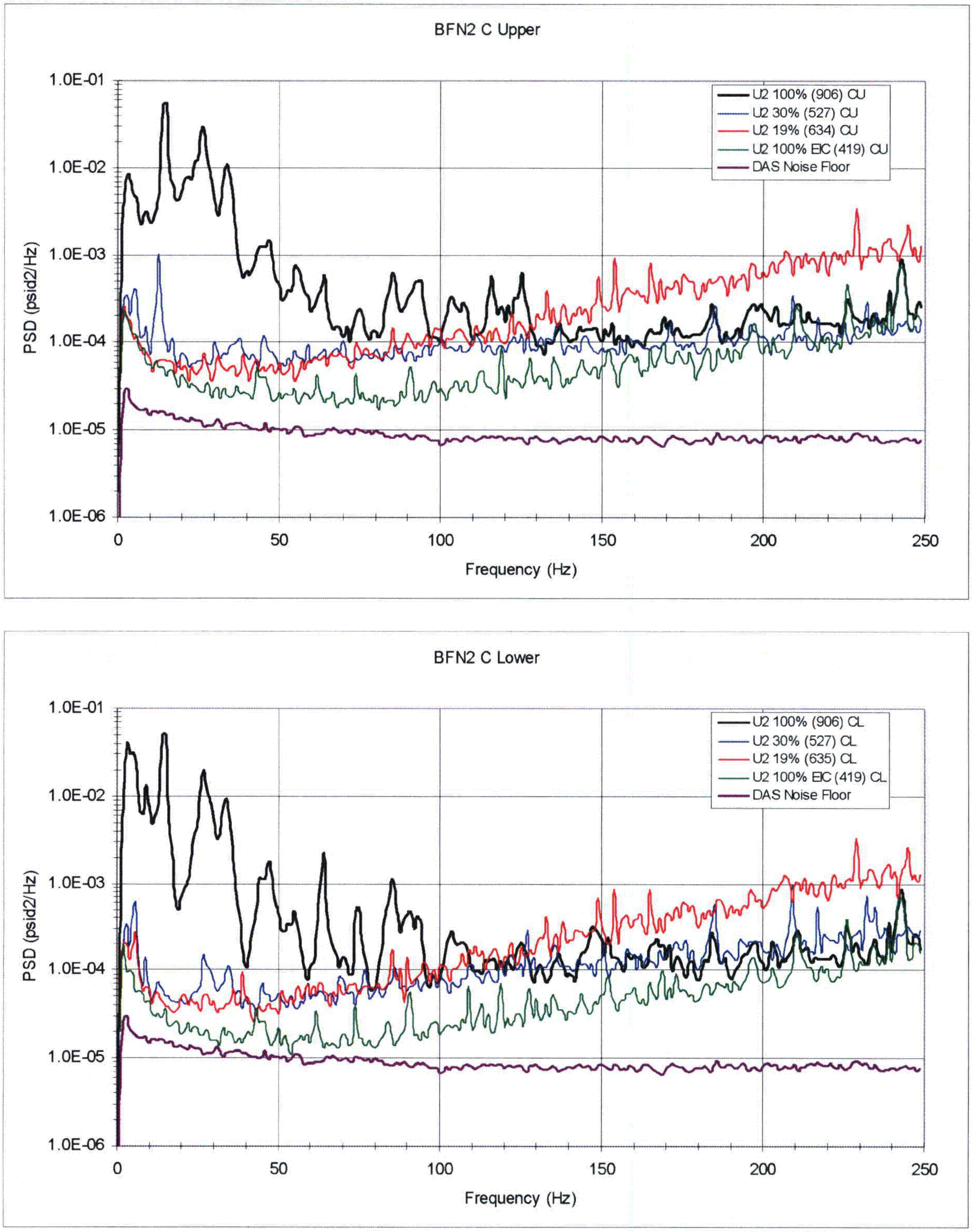

Figure EMCB.147-1c: Unit 2 Data MSL C

NON-PROPRIETARY INFORMATION

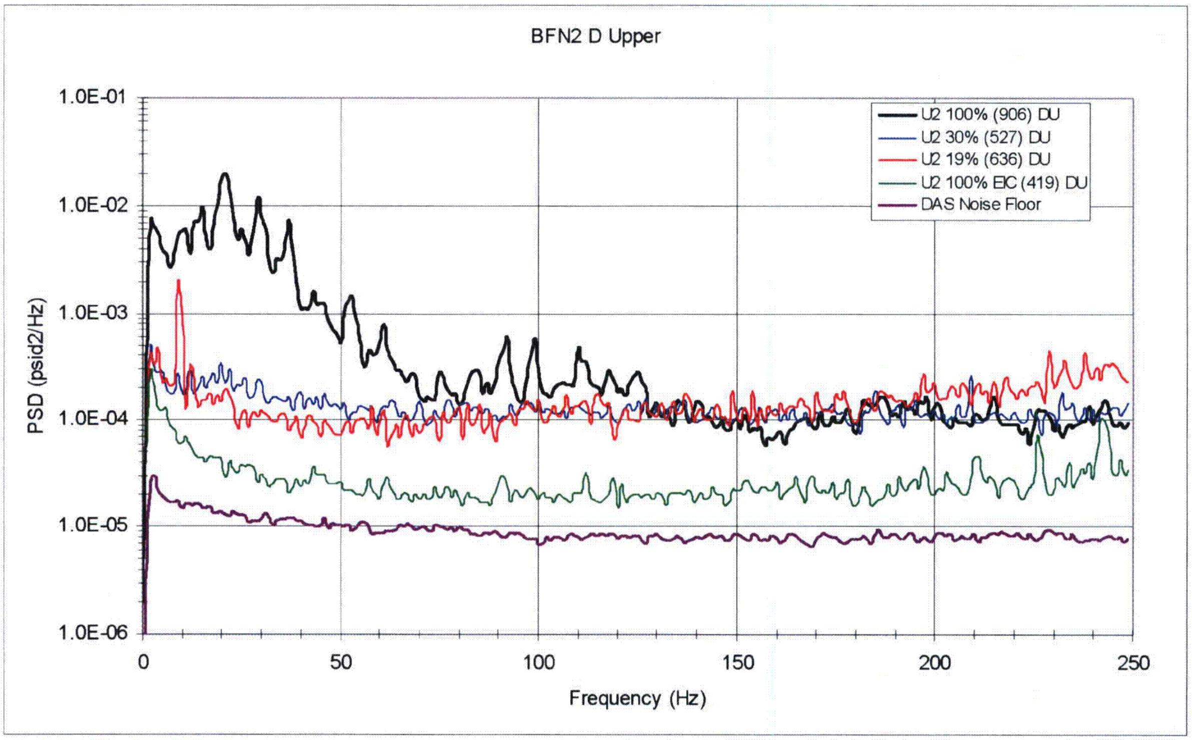

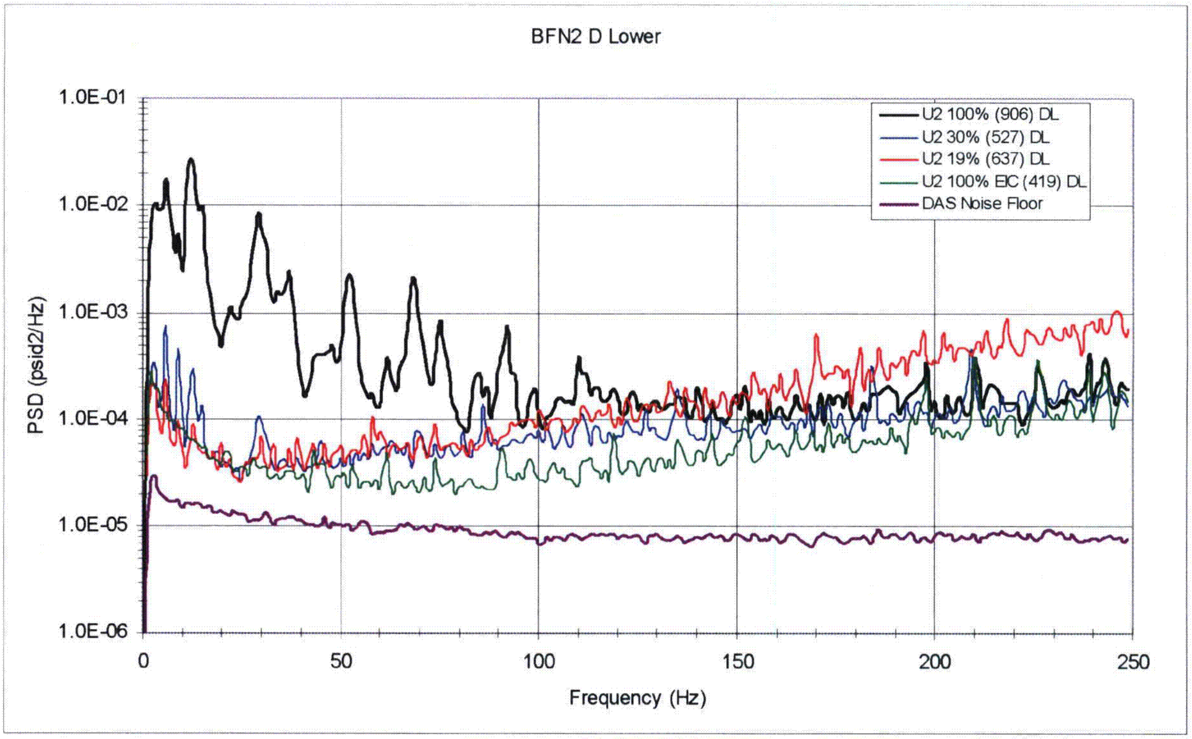

Figure EMCB.147-1d: Unit 2 Data MSL D

NRC RAI EMCB.184/148 (Unit 1/Unit 2)

Explain why two different power levels (9 percent in Unit 1 and 19 percent in Unit 2) are considered for pressure measurements at low-flow conditions.

TVA Response to EMCB.184/148 (Unit 1/Unit 2)

Use of low flow pressure measurements to determine the contributions from non-acoustic sources was developed subsequent to MSL strain gage measurements during the BFN Unit 1 and Unit 2 startups for the current operating cycles. As such, specific measurements at low flow were not planned as part of the testing. Therefore, low flow MSL strain gage measurements are limited to available data taken during power ascension, the lowest of which were 9% for Unit 1 and 19% for Unit 2.

NRC RAI EMCB.185/149 (Unit 1/Unit 2)

In the event that noise removal from the MSL strain gage signals is not justifiable in Units 1 and 2, discuss what additional structural modifications to the Unit 1 and/or Unit 2 dryers would TVA consider that would lead to acceptable alternating stress ratios.

TVA Response to EMCB.185/149 (Unit 1/Unit 2)

TVA has performed preliminary Unit 1 and Unit 2 stress analyses with noise retained and evaluated the resulting stresses in order to determine the impact on dryer components relative to the goal of maintaining a SR-a of 2.7 at CLTP to support approval for EPU operation. There are 9 locations on Unit 1 and 14 on Unit 2 where the SR-a would be less than 2.7. Options have been identified for each location involving one or more approaches. More rigorous analysis must be completed to confirm a viable success path for all of the locations.

- Physical modifications
  Modifications being studied include additional weldments, re-enforcement strips and additional gussets, all of which are analysis dependent.

  Unit 1 has three locations (with 4 to 12 associated symmetrical locations) which involve modifications. Some of these modifications would require access underneath the dryer and may not be feasible from the standpoint of industrial safety and radiation dose.

  Unit 2 has three locations (with 2 to 16 associated symmetrical locations) which involve modifications. Some of these modifications would require access underneath the dryer and may not be feasible from the standpoint of industrial safety and radiation dose.

- Reduced bias/uncertainty factor in the frequency range of 109 to 113 Hz
  TVA has been applying an increased bias and uncertainty factor of 75% over the 109 to 113 Hz frequency range corresponding to the expected frequency of safety relief valve (SRV) resonance. However, with the installation of Acoustic Side Branches (ASBs), no significant SRV resonance is expected.

- Use of a 1.4 weld factor for full penetration groove welds
  Currently, a 1.8 weld factor is used irrespective of the type of weld.

- The use of additional submodels
  New submodels will be developed for locations whose configuration or stress distribution is different from the submodels previously developed. In those instances, the full

process as described in the response to RAI EMCB.180 in the June 16, 2008 submittal will need to be performed.

NRC RAI EMCB

In the stress assessment of the BFN Unit 1 steam dryer, TVA has employed substructure modeling, as shown in Structural Integrity Associates calculation (File No. 0006982301), for estimating the complete 3-dimensional stress distribution at the two locations having the lowest alternating stress ratios: (1) the intersection between the bottom of the inner hood, stiffener and base plate, and (2) the bottom of the skirt/drain channel junction. For the first location, TVA simulates the stress profile of the full model analysis by applying static loading on a short section of the stiffener. For the second location, TVA applies the prescribed displacement at specific intervals along a vertical line in the drain channel and performs the 3-D analysis iteratively by changing the location of the vertical line until the stress profile matches the stress profile of the full model analysis. Then, for each location, TVA determines the largest ratio of the (Pm + Pb) stress intensity from the sub-model against that from the full model analysis and applies it to the stresses at the corresponding location in the steam dryer analysis. Given the above, provide a response to the following questions:

NRC RAI EMCB.186 (Unit 1 only)

Justify the use of static sub-model analysis results for modifying the dynamic stress analysis results for the Unit 1 steam dryer, which is subjected to fluctuating pressure loads.

TVA Response to EMCB.186 (Unit 1 only)

The loadings and boundary conditions used in the shell submodel to create the weld connections include the dynamic effect as determined in the full 3D steam dryer model. Since the same loadings and boundary conditions are used in the solid submodel, which has the same dimensions as the shell submodel, the solid submodel also includes the dynamic effect similar to those in the full 3D model. The approach can be viewed as performing the dynamic analysis by an equivalent quasi static analysis with a dynamic amplification factor on the loads. The basis for this approach is explained as follows:

First, the stresses at the weld connections of interest are extracted from the full 3D model solution at the point in time where the stresses in the weld connection are the maximum under the transient loadings. For the hood stiffener submodel, the extracted stress profile covered a vertical length of approximately 17 inches in the weld connection from the bottom of the stiffener. For the drain channel submodel, it covered the entire vertical length of the drain channel-to-skirt connection. Since these stresses are obtained from the dynamic solution of the full 3D shell model subjected to fluctuating acoustic pressure loads, they clearly reflect the dynamic behavior of the full dryer.

Next, loads and boundary conditions are statically applied to the shell submodels in an iterative process until the magnitude and distribution of weld connection stresses in the submodel are similar to the extracted stresses from the full 3D shell model dynamic. By deduction, the loading and boundary conditions used in the shell submodel to recreate these weld connection stresses include the dynamic effects of the entire steam dryer. Since the same loadings and boundary conditions are also used in the solid submodel, which has the same dimensions as the shell submodel, it is concluded that the solid submodel also includes dynamic effects equivalent to those in the full 3D model. Thus, the use of static shell and solid submodel solutions as described above is a justified approach for detailed evaluation of the weld connections because the resulting stresses reflect the dynamic behavior of the full dryer, including any effects local to the submodel itself.

NRC RAI EMCB.187 (Unit 1 only)

Figure 4.1 of the SIA calculations shows that 1,000 lb force is applied to the stiffener. Please explain why no loads are applied to Edges A, B and C? TVA is requested to provide the final applied load to the sub-model and a comparison of the resulting sub-model stress profile and the full model stress profile.

TVA Response to EMCB.187 (Unit 1 only)

As explained in the response to RAI EMCB.186, the loadings and boundary conditions are selected with the following requirements

(a) The weld connection stress in the shell submodel matches CDI full model weld connection stress.

(b) The same loading and boundary conditions in the shell submodel have to be used in the solid submodel.

Any combination of boundary conditions or loading conditions can be applied to Edges A, B and C in the shell submodel as long as it provides a matching stress condition in the weld connection in the shell submodel. It should also be noted that the stresses in areas far away from the weld connection are not relevant in this evaluation.

To match the shell submodel stress profile with the full 3D shell model stress profile, the iterations are made on two parameters:

1. The magnitude of the load.

2. The stiffener height at which the load is evenly applied.

In the final iteration, the applied load is 267.2 lbs, evenly distributed over 1.75 inches of the stiffener height. Figure 4.1 of the SIA calculation shows the applied load 1,000 lb, which is the initial load used at the start of iteration. The actual load that corresponds to the full 3D shell model stress is 267.2 lbs.

The comparison of the stress profile in the shell submodel and the stress profile of the CDI full 3D shell model is shown in the Figure EMCB.187-1.

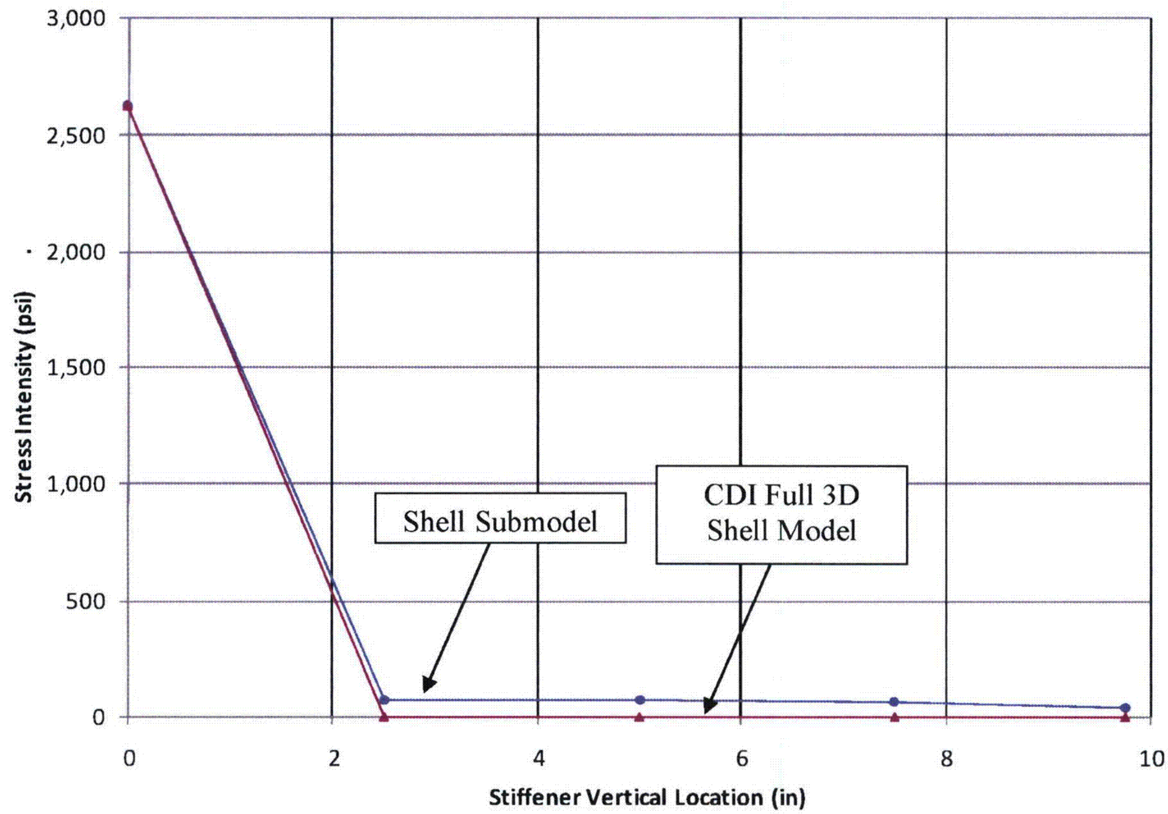

Figure EMCB.187-1: Stiffener Shell Submodel and Full 3D Shell Model Stress Profile Comparison

The stress profile comparison is focused on the 5 nodes closest to the location of interest, which is located at the bottom of the stiffener (i.e., at 0 inch vertical location). Nodes further away from the location of interest have diminished and insignificant influence on the maximum stress at the bottom. As the stress drops off very quickly away from the highest stress location located at the bottom of the stiffener, it is considered that the stress profile comparison up to the first 5 nodes is sufficient.

When the comparison is judged to be reasonable, the same set of loadings and boundary conditions are applied to the solid submodel to obtain a better detailed stress distribution in the weld connection since the complexity of the weld configuration is included in the solid submodel.

NRC RAI EMCB.188 (Unit 1 only)

Explain the application of the prescribed displacements at the skirt/drain channel junction. Also explain the iterative analysis approach for the sub-model of the skirt/drain channel junction.

TVA Response to EMCB.188 (Unit 1 only)

The mode of loading application in the skirt/channel submodel is different than for the stiffener submodel. This was necessary because after many attempts, the application of the force loadings did not produce a satisfactory match in the weld connection stresses between the shell submodel and the full 3D steam dryer model.

NON-PROPRIETARY INFORMATION

As described in the responses to RAIs EMCB.186 and EMCB.187, the mode of loading is not restricted to a particular type (i.e., force/moment versus displacement/rotation) as long as it produces a match in the weld connection stress. It was then switched to the application of displacements instead of forces at the location as shown along Line C in Figure EMCB.188-1.

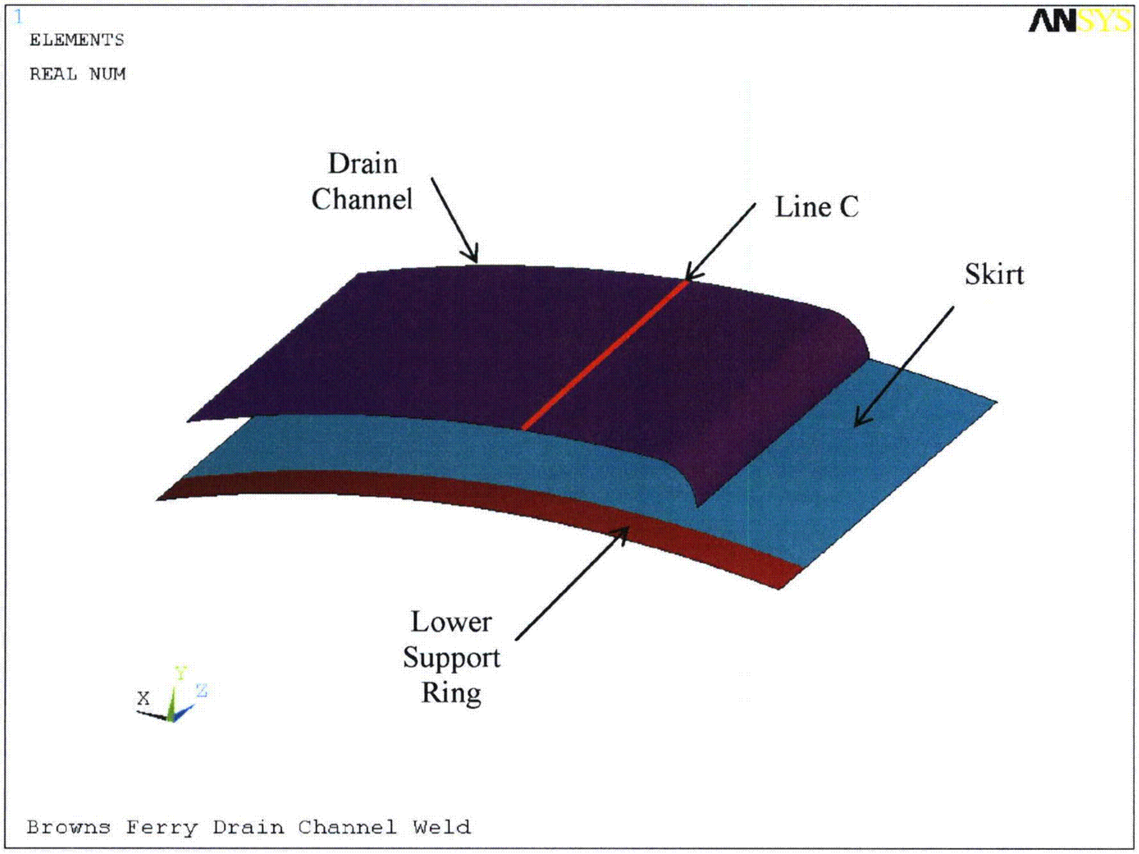

Figure EMCB.188-1: Drain Channel Model Applied Load

<u>Applied Load</u>

Along Line C: Imposed outward radial displacements along the line at 1 inch regular intervals.

<u>Iterative Approach</u>

The following 2-step iterative approach is used:

<u>Step 1 - Iterate on Line C Location</u>

a) Arbitrarily select a vertical line (Line C as shown in Figure EMCB.188-1) located in the drain channel.

b) Proceed to Step 2 to iterate on the imposed displacements until the best match of stress profile is obtained for the selected vertical line. The initial maximum imposed displacement is 0.2 inches.

Step 2 - Iterate on The Imposed Displacements

a) Impose a set of prescribed outward radial displacements, at 1 inch regular intervals along a vertical line (identified as Line C in Figure EMCB.188-1). This vertical line is identified in Step 1.

b) Compute the stress intensity along the drain channel/skirt interface.

c) Compare the shell submodel stress profile and the full 3D shell model stress profile.

d) Repeat sub-steps a) to c) by varying the prescribed displacement in sub-step a). This iterative process is repeated until the best match of stress profile is obtained for this chosen Line C.

This 2-step iterative approach is repeated until a satisfactory match is obtained for the stress profiles between the shell submodel and the full 3D shell model.

NRC RAI EMCB.189 (Unit 1 only)

Provide the final magnitude of imposed displacement along with the location and a comparison of the resulting sub-model stress profile and the full model stress profile.

TVA Response to EMCB.189 (Unit 1 only)

A plot of the final imposed drain channel/skirt displacements is provided in Figure EMCB.189-1.

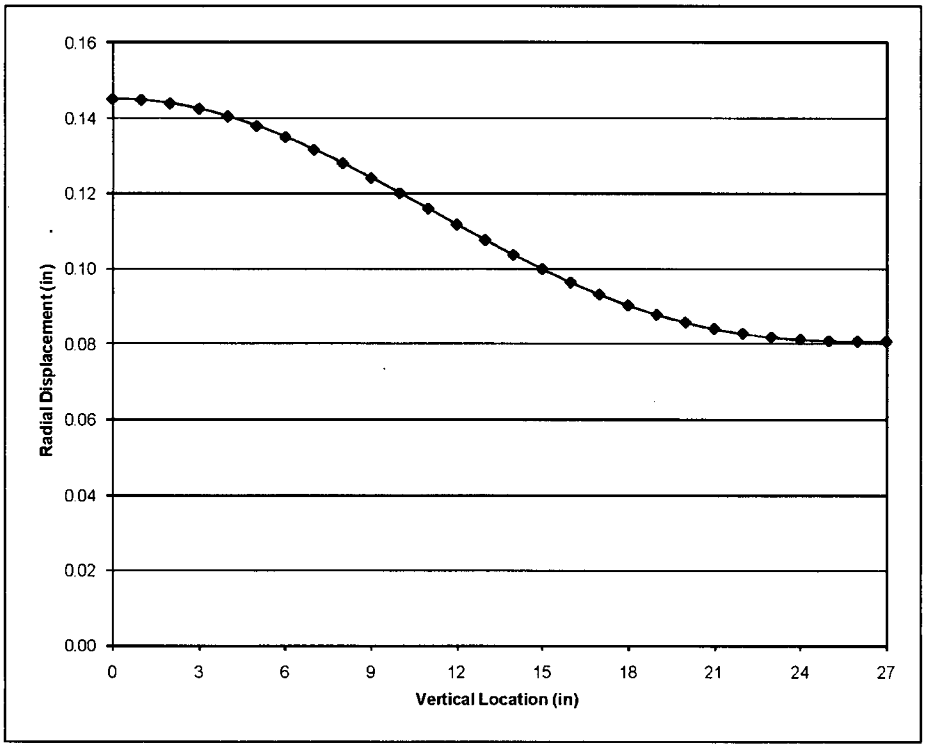

Figure EMCB.189-1: Drain Channel Imposed Displacements

The imposed displacements are in the outward radial direction along the vertical Line C (see Figure EMCB.188-1). The maximum magnitude of displacement is 0.145 inch at the bottom, reducing to 0.08 inch at the top of the modeled drain channel. Figure EMCB.189-2 shows the comparison of the stress profile.

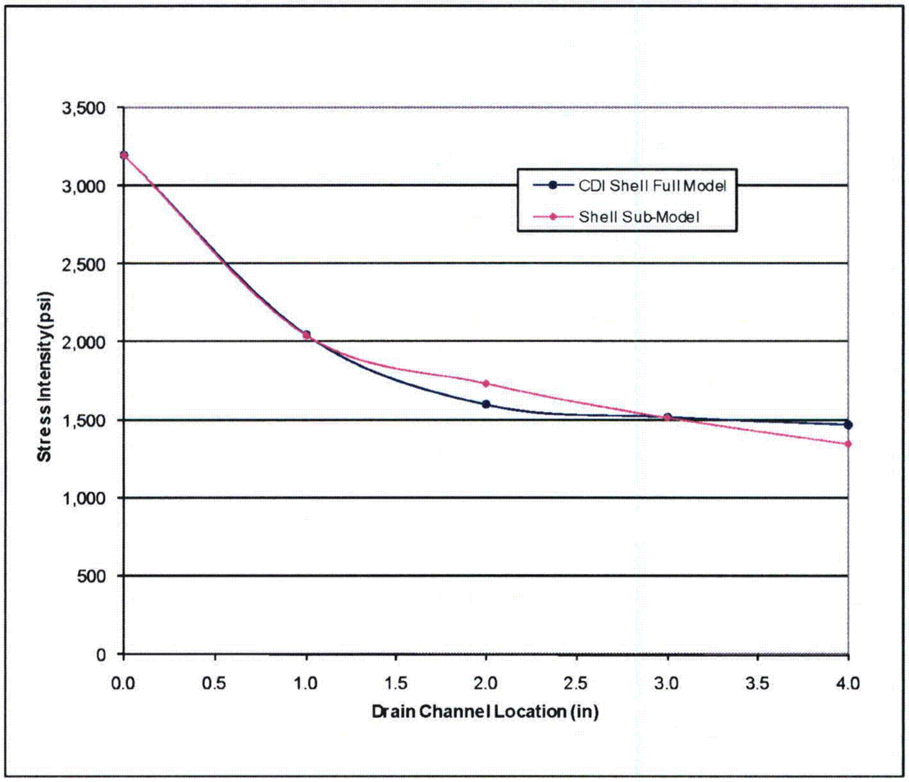

Figure EMCB.189-2: Drain Channel Stress Profile Comparison

The stress profile comparison is focused on the 5 nodes closest to the location of interest, which is located at the bottom of the drain channel (i.e., at 0 inch vertical location). Nodes further away from the location of interest have diminished and have insignificant influence. It is considered that the stress profile comparison up to the first 5 nodes is sufficient.

NRC RAI EMCB.190 (Unit 1 only)

Provide confirmation that the stress correction factors computed using sub-structure modeling are independent of the mesh sizes of the shell and the solid models.

TVA Response to EMCB.190 (Unit 1 only)

As described in the response to RAI EMCB.186, the two submodels serve different purposes. The shell submodel is to match the weld connection stress while the solid submodel is to get a better stress prediction in the weld connection. Therefore, the mesh sensitivity is not critical in the shell submodel because its purpose is to obtain a set of boundary conditions and loadings in the shell model such that these can be applied to the solid submodel provided the connection stress in the shell model matched with the 3D full shell model. No matter what mesh size is used in the shell submodel, the critical stress (i.e., the stress at the bottom tip of the drain channel) to be used in the stress correction factor has to be the same as the critical stress in the full 3D shell model since this is the sole purpose of the shell submodel. Given that set of boundary and loading conditions obtained from the shell submodel where the critical stress has matched with the results in the full 3D shell model, it has to be confirmed that under the same boundary and loading conditions, the mesh size in the solid submodel is sufficient such that the linearized P_m+P_b could not deviate significantly.

For the mesh sensitivity study, the model selected for comparison is the drain channel since this model is more complex. The number of elements through the thickness of the drain channel is increased from 6 elements to 8 elements for both the drain channel and the skirt. The linearized P_m+P_b at all the paths are then obtained. The comparison of stress intensities is shown in the following table.

Table EMCB.190-1 : Drain Channel Pm + Pb Stress Intensity Comparison

Path #	Original Mesh (psi)	Refined Mesh (psi)	Difference (%)
1	765.2	764.4	-0.1
2	837.4	851.0	1.6
3	1859.9	1871.3	0.7
4	339.5	338.9	-0.2
5	227.0	229.3	1.0
6	1029.0	1037.4	0.8
7	812.3	810.1	-0.3
8	549.0	552.1	0.6
9	790.6	789.8	-0.1
10	1022.5	1038.4	1.6
11	1858.9	1871.3	0.7
12	2585.7	2591.4	0.2

The above comparison shows that differences vary from -0.3% to 1.6%, a maximum increase of less than 2%. The largest stress intensity is associated with Path #12, which shows an increase of only 0.2%. These insignificant stress differences show that the mesh size used in the analysis is acceptable and further mesh refinement is not necessary.

NRC RAI EMCB.191 (Unit 1 only)

In response to NRC RAI EMCB.171/139, TVA states that at a small number of frequencies, the [[ ]] damping actually increases the peak responses as shown in Figure EMCB.171/139-1. Explain how such increases are physically compatible with a displacement driven modal response.

TVA Response to EMCB.191 (Unit 1 only)

[[ ]], a representative example involving a simply supported beam of length L, flexural stiffness EI, and mass per unit length $m=\rho S$, where ρ is the density and S the cross-sectional area, is considered. Let w be the normal displacement and suppose the motion to be subject to a normal damping force per unit length, $f_d = C\dot{w}$. [[

]] If f is the applied normal acoustic load, then the virtual work statement governing the beam response is

$$\int_0^L EIw''\,\bar{w}''\,dx = \int_0^L (f - C\dot{w} - m\ddot{w})\,\bar{w}\,dx \qquad (191\text{-}1)$$

where $\bar{w}$ denotes a virtual displacement. For a simply supported beam with no motion of the endpoints, the first response mode is accurately represented by $w=A(t)\sin(\pi x/L)$ where A is the amplitude. Adopting a Rayleigh-Ritz approach, $\bar{w} = \bar{A}\sin(\pi x/L)$ and inserting for w and $\bar{w}$ into the preceding relation

$$m\ddot{A} + C\dot{A} + EI(\pi/L)^4 A = \frac{2}{L}\int_0^L f\sin(\pi x/L)\,dx \qquad (191\text{-}2)$$

For the case of a constant force f = F, this becomes

$$\ddot{A} + 2\zeta\omega_n\dot{A} + \omega_n^2 A = \frac{4F}{\pi m} \qquad (191\text{-}3)$$

where

$$\omega_n^2 = \frac{EI}{m}(\pi/L)^4 \quad \text{and} \quad 2\zeta\omega_n = C/m \qquad (191\text{-}4)$$

The frequency response function is obtained by assuming harmonic motion, $F = \tilde{F}e^{i\omega t}$ and $A = \tilde{A}e^{i\omega t}$, so that

$$\frac{A}{F} = \frac{4}{\pi m\left(\omega_n^2 - \omega^2 + 2\zeta\omega_n i\omega\right)} \qquad (191\text{-}5)$$

The response amplitude

$$\frac{|A|}{|F|} = \frac{4}{\pi m\omega_n^2\sqrt{(1-r^2)^2 + (2\zeta r)^2}} \qquad (191\text{-}6)$$

where $r=\omega/\omega_n$. One can now compare this amplitude response against the one obtained with zero damping

$$\frac{|A(\zeta)|}{|A(\zeta=0)|} = \frac{|1-r^2|}{\sqrt{(1-r^2)^2 + (2\zeta r)^2}} < 1, \quad (\zeta r>0) \qquad (191\text{-}7)$$

This ratio is less than unity for all nonzero damping and frequencies, which implies that the damped response amplitude is always less than or equal to the undamped response. Since stress is proportional to the response amplitude (the peak bending stress,

$\sigma = Ew''_{max}t/2 = E\pi^2At/2L^2$, where t is the element thickness), the implication is that the stress for the damped beam is everywhere less than in the undamped one.

Now consider the same beam with zero applied force, f = 0, but with both ends moved by a prescribed displacement $w_0(t)$. Let the beam displacement be approximated by, $w = w_0(t) + A\sin(\pi x/L)$. The virtual displacement due to deformation is the same as before, $\bar{w} = \bar{A}\sin(\pi x/L)$ (a uniform virtual displacement analogous to w_0 can also be included which leads to the expression for the normal reaction forces at the beam supports). Substituting for w and $\bar{w}$ into the virtual work statement results in

$$m\ddot{A} + C\dot{A} + EI(\pi/L)^4 A = -\frac{4}{\pi}(C\dot{w}_0 + m\ddot{w}_0) \qquad (191\text{-}8)$$

Again assuming harmonic motion with $w_0 = \tilde{w}_0 e^{i\omega t}$

$$\frac{\tilde{A}}{\tilde{w}_0} = -\left(\frac{4}{\pi}\right)\frac{2\zeta\omega_n i\omega - \omega^2}{\omega_n^2 - \omega^2 + 2\zeta\omega_n i\omega} = -\left(\frac{4}{\pi}\right)\frac{2\zeta ir - r^2}{1 - r^2 + 2\zeta ir} \qquad (191\text{-}9)$$

If, as previously, one now forms the ratio between the damped and undamped response amplitudes, one obtains

$$\frac{|\tilde{A}(\zeta)|}{|\tilde{A}(\zeta = 0)|} = \sqrt{\frac{r^4 + (2\zeta r)^2}{(r^2 - 1)^2 + (2\zeta r)^2}} \cdot \frac{|r^2 - 1|}{r^2} \qquad (191\text{-}10)$$

It is readily shown that this ratio exceeds unity when $r^2 < ½$ implying that in this frequency range the displacement, and thus also stress, for the damped system is higher than for the undamped one.

Though demonstrated for a relatively simple problem, the same principle holds for more complex situations. Note furthermore that for multi-degree, it is possible to increase stress even in a force-driven case owing to mode combination. To illustrate, one can consider the stress σ, at a point to be the linear supposition of two modal contributions, $\sigma = \sigma_1\eta_1 + \sigma_2\eta_2$, where η_i are the modal amplitudes and σ_i is the stress contributions of each mode. In general σ_1 and σ_2 are signed quantities. Suppose $\sigma_2 = -(1/2)\sigma_1$ and that in the undamped case $\eta_1 = \eta_2 = 1$. Then $\sigma=(1/2)\sigma_1$ without damping. Next suppose that with the introduction of damping, the modal amplitudes reduce to η_1=5/6 and η_2=1/3 (note that, in general, damping will reduce the modal response amplitudes by different amounts). The stress then changes to $\sigma=(2/3)\sigma_1$ which is higher than in the undamped case even though both modal amplitudes have diminished.

NRC RAI EMCB.192/150 (Unit 1/Unit 2)

Provide the following information about the planned acoustic side branches (ASBs) for Units 1 and 2, including validation results:

(a) Identify which safety/relief valves the ASBs will be installed on;

(b) Provide the lengths of the various ASBs and the acoustic resonance frequencies associated with them;

(c) Describe the power level(s) at which these (new) acoustic resonances will be excited. If the new resonances are excited, discuss whether it will be locked in;

(d) Provide the estimated minimum alternating stress ratio of the dryer at flow conditions corresponding to the acoustic resonance of the standpipe-ASB combination; and,

(e) Address whether the ASBs will be designed by means of the scale-model test, if so provide the corresponding test results for review.

TVA Response to EMCB.192/150 (Unit 1/Unit 2)

(a) ASBs will be installed on the nine SRVs that are in the main steam flow path. Four SRVs are located on the MSL dead legs and will not be modified with ASBs. Figure EMCB.192/150-1 shows a typical placement of ASBs for BFN. This is a preliminary drawing and final orientation of the ASBs on each unit may vary.

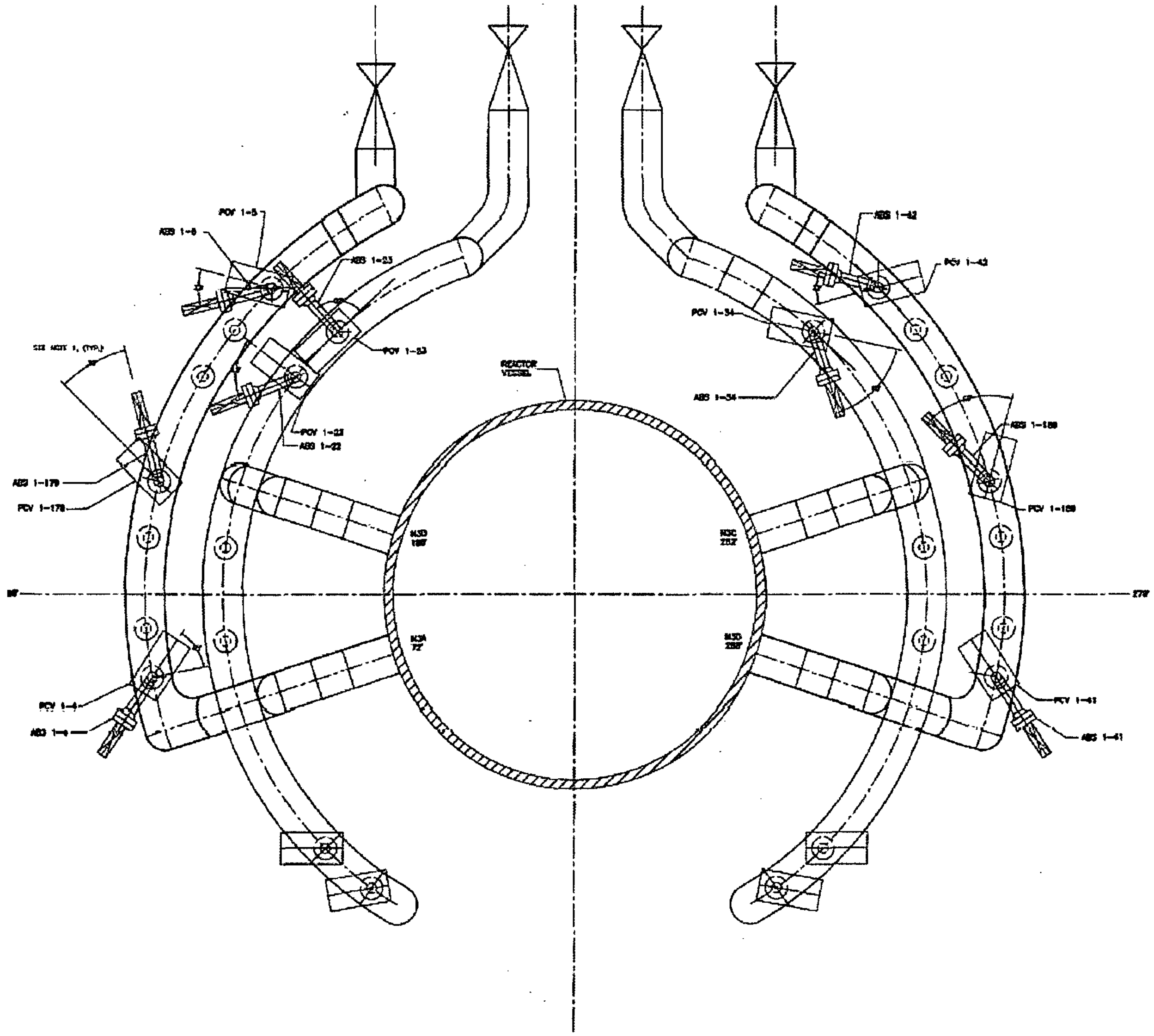

Figure EMCB.192/150-1: Illustration of Typical Placement of ASBs

(b) The BFN ASBs will be the same nominally 24 inch long side branch. The internal canister consists of compressed screening material used to dampen and attenuate the resonance energy. This is the same design as developed and tested for Quad Cities. The ABS will move the resonance frequency for the SRV from a nominal 106-110 Hz to 96.5 Hz (calculated) to 100.4 Hz (tested). The ASB without wire dampening material typically lowers the resonant frequency of the standpipe/valve system, because it effectively lengthens the acoustic column. Once damping material is inserted into the ASB, the resonant frequency is effectively eliminated due to the fact that the wire screens add large damping to the system. While the term "resonant frequency" is used for ASBs, an amplified response in the traditional sense does not occur.

(c) The new resonance frequency of the SRVs with ASBs installed would experience onset around 83% CLTP.

(d) BFN scale model testing with the ASBs is in progress to confirm the effectiveness of the ASBs in the BFN steam line configuration. The results of the testing will be used to determine the effect on the stress analysis results. The results of this analysis will be provided by September 19, 2008.

(e) The 24 inch ASB design developed for Quad Cities was selected based on the demonstrated results at Quad Cities. BFN scale model testing is in progress to confirm the effectiveness of ASBs in the BFN steam line configuration.

NRC RAI EMCB.151 (Unit 2 only)

In the response to RAI EMCB.130/97, TVA provides a comparison between the Unit 3 MSL strain gage signals (with acoustic vibration suppressor(AVS)) with the corresponding Unit 1 signals (without AVS), which demonstrate the effectiveness of AVS in suppressing 218 Hz signal. Provide a similar comparison between Unit 3 and Unit 2 MSL signals so that the staff can further evaluate the effectiveness of AVS.

TVA Response to EMCB.151 (Unit 2 only)

The figures provided in the response to RAI EMCB.130/97 in the June 16, 2008 submittal have been updated with information from Unit 2 in Figures EMCB.151-1 through 5. In these figures, data from the Unit 3 single strain gages at 100 percent power with AVSs installed are compared with data from Unit 1 and Unit 2 single strain gages at 100 percent power at equivalent locations with no AVSs installed. In cases where the Unit 1 or Unit 2 strain gage at the same location was inoperable, the diametrically opposite strain gage was used for comparison. In Channel 1, data was not available for Unit 2. Line noise and reactor recirculation system frequencies were filtered. The 218 Hz signal was not filtered on any unit.

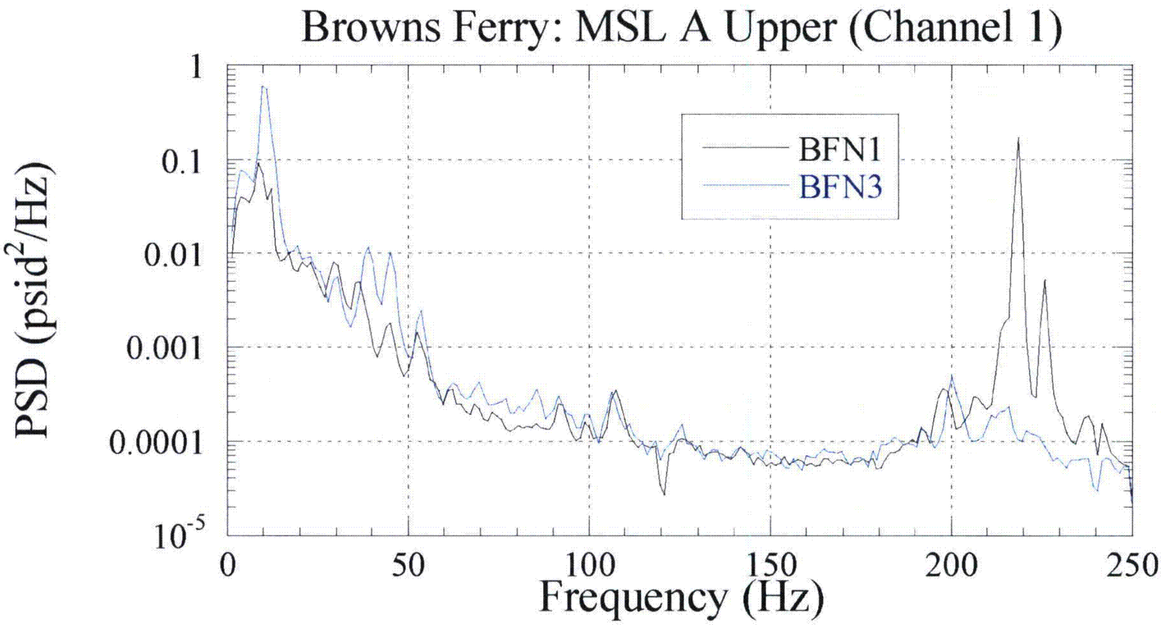

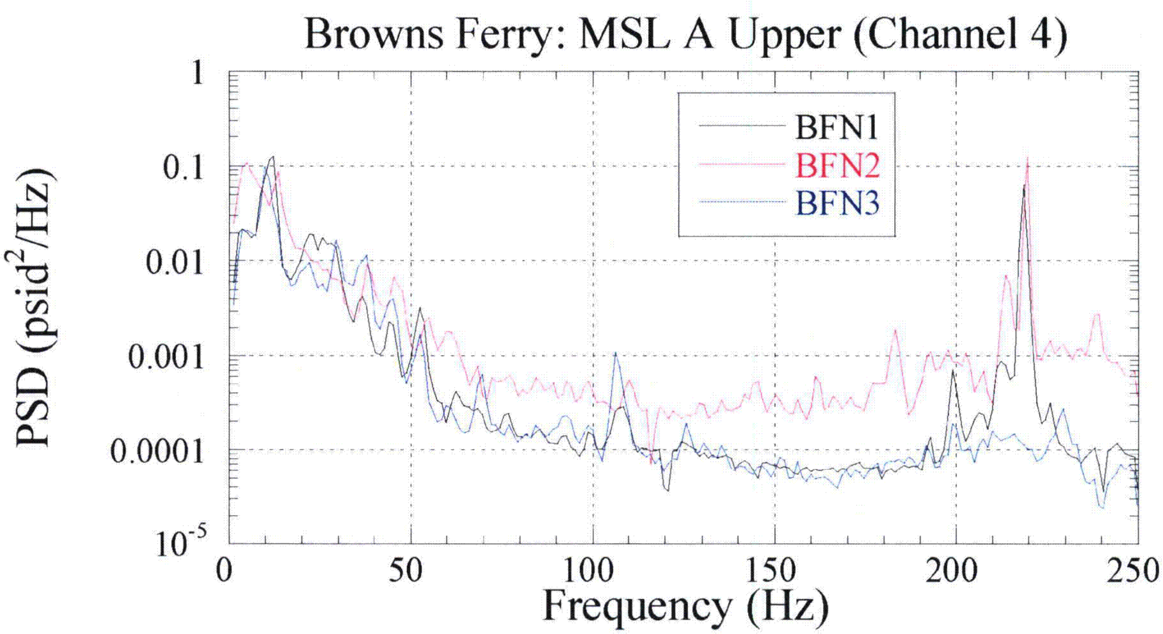

Figure EMCB.151-1: PSD comparison of pressure measurements on MSLs

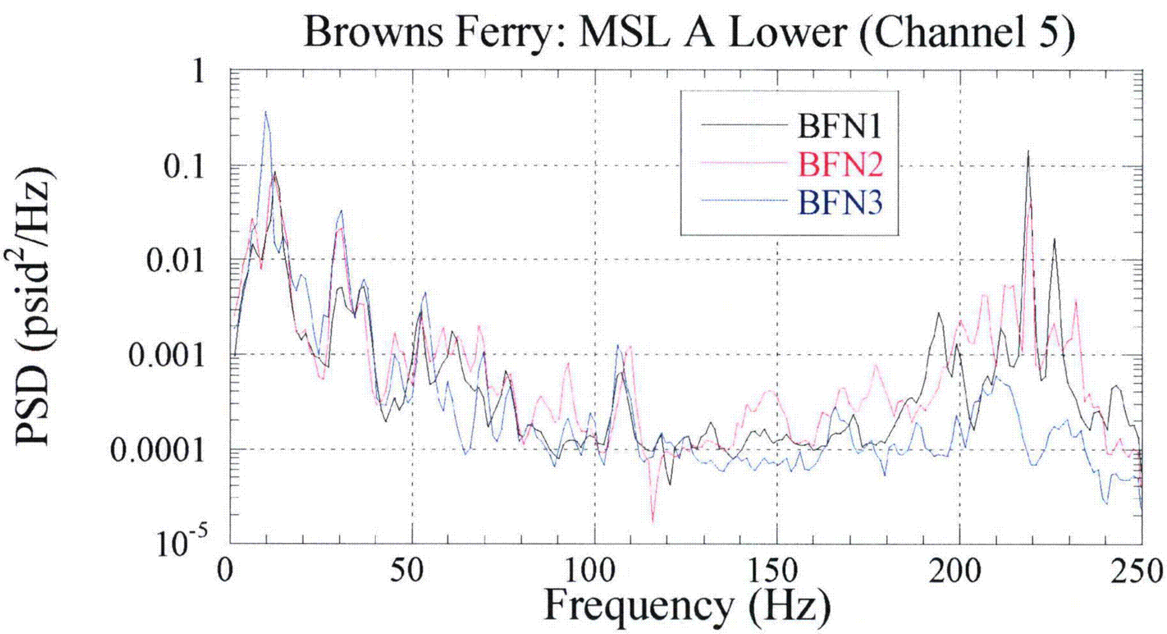

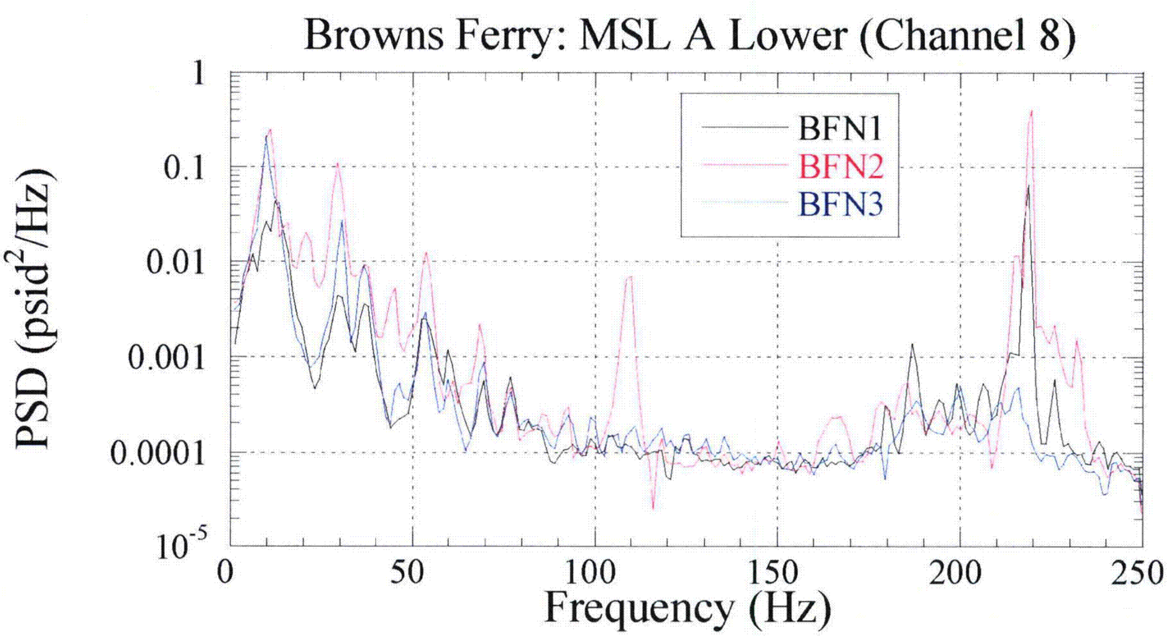

Figure EMCB.151-2: PSD comparison of pressure measurements on MSLs

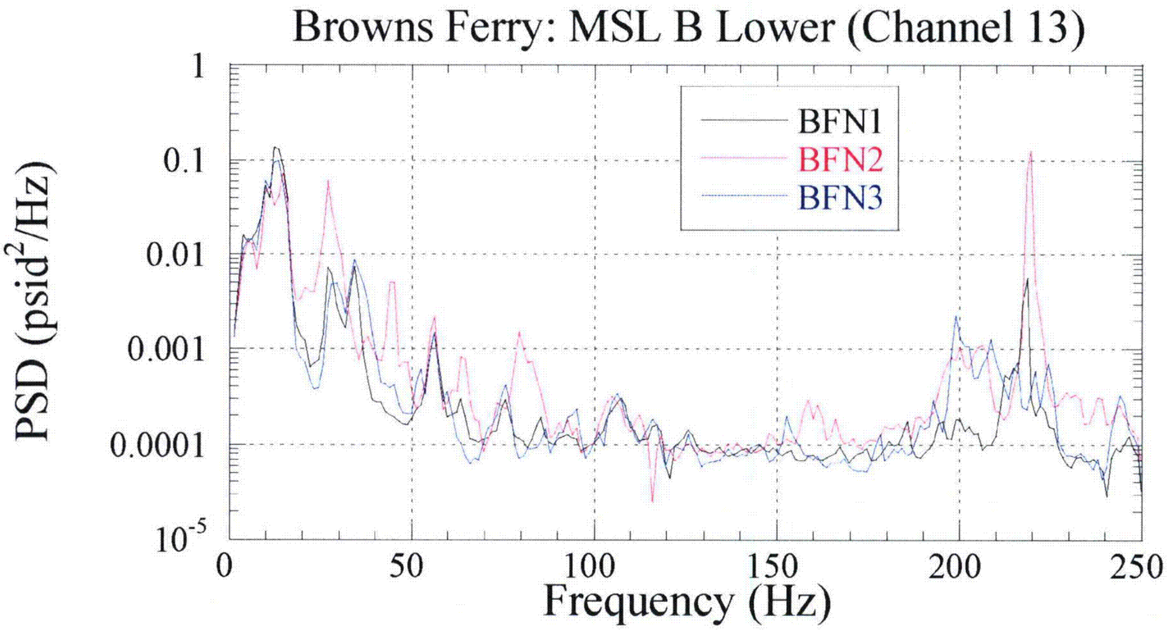

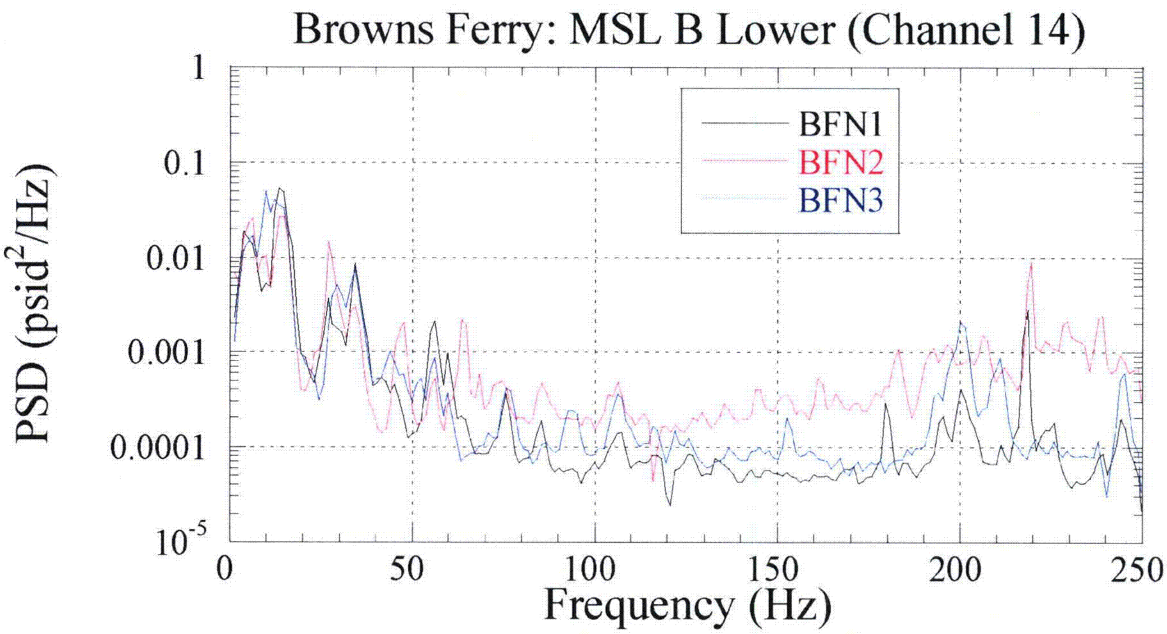

Figure EMCB.151-3: PSD comparison of pressure measurements on MSLs

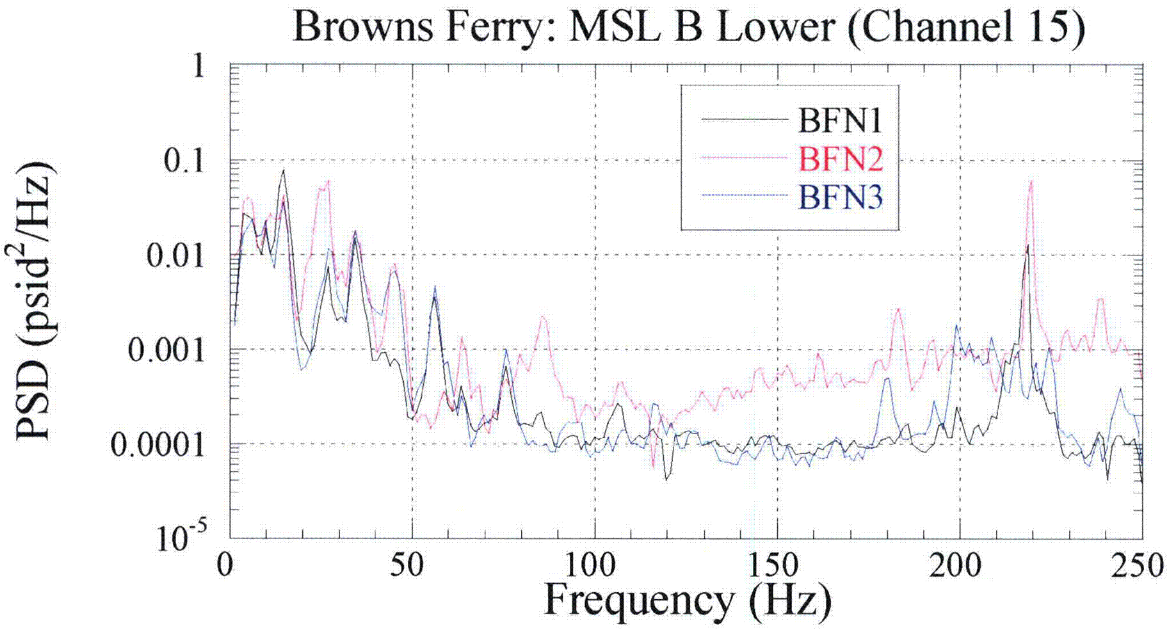

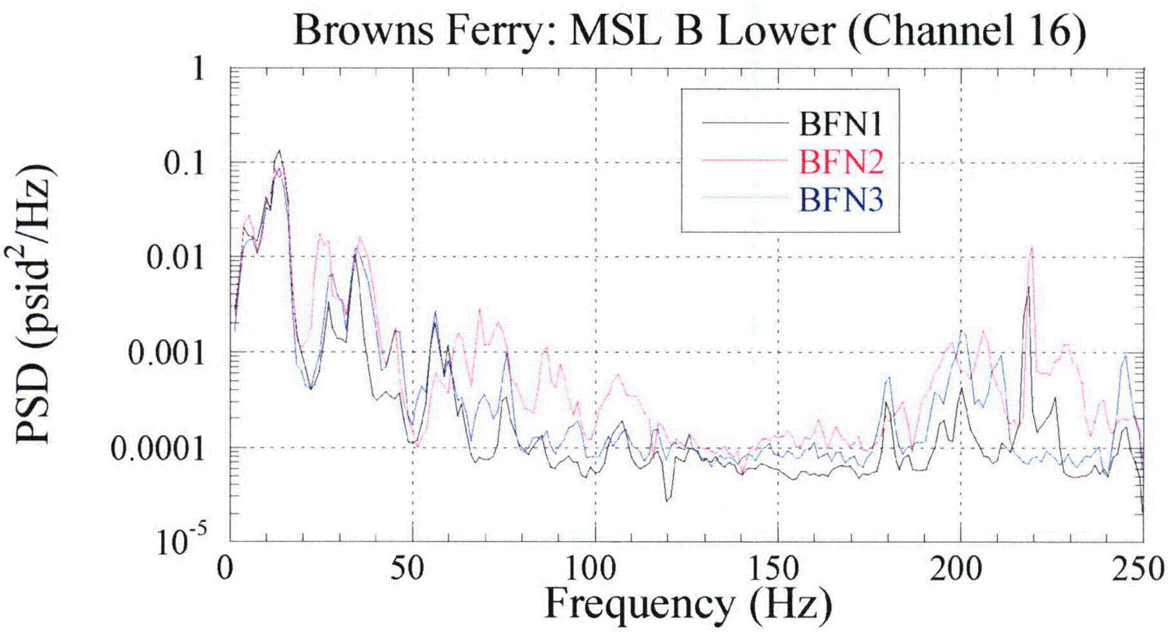

Figure EMCB.151-4: PSD comparison of pressure measurements on MSLs

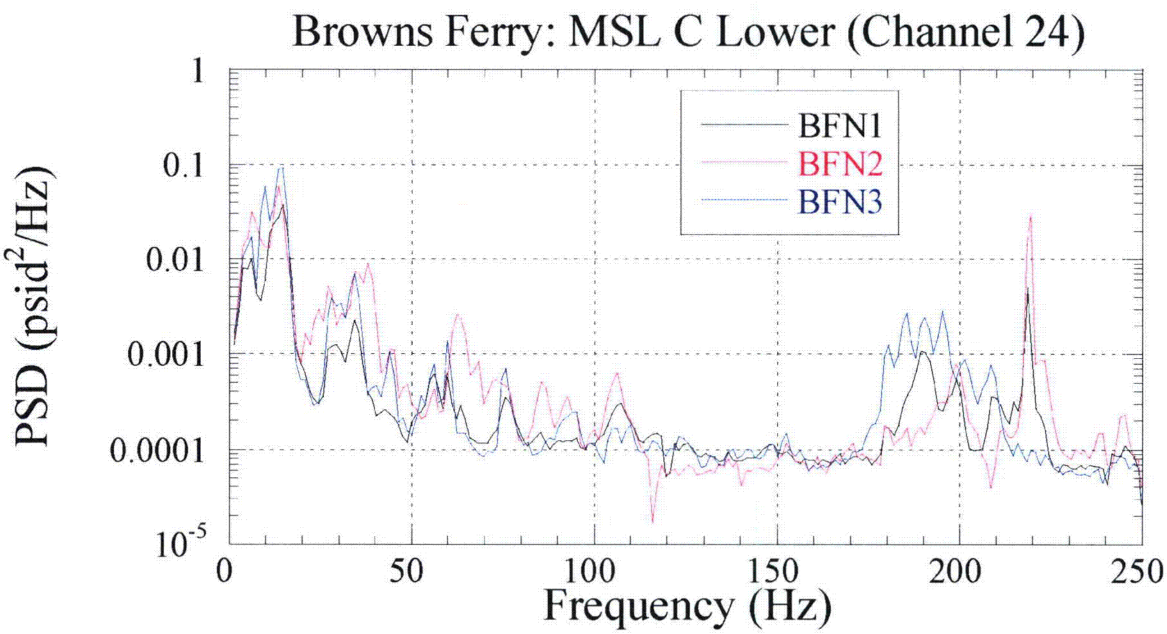

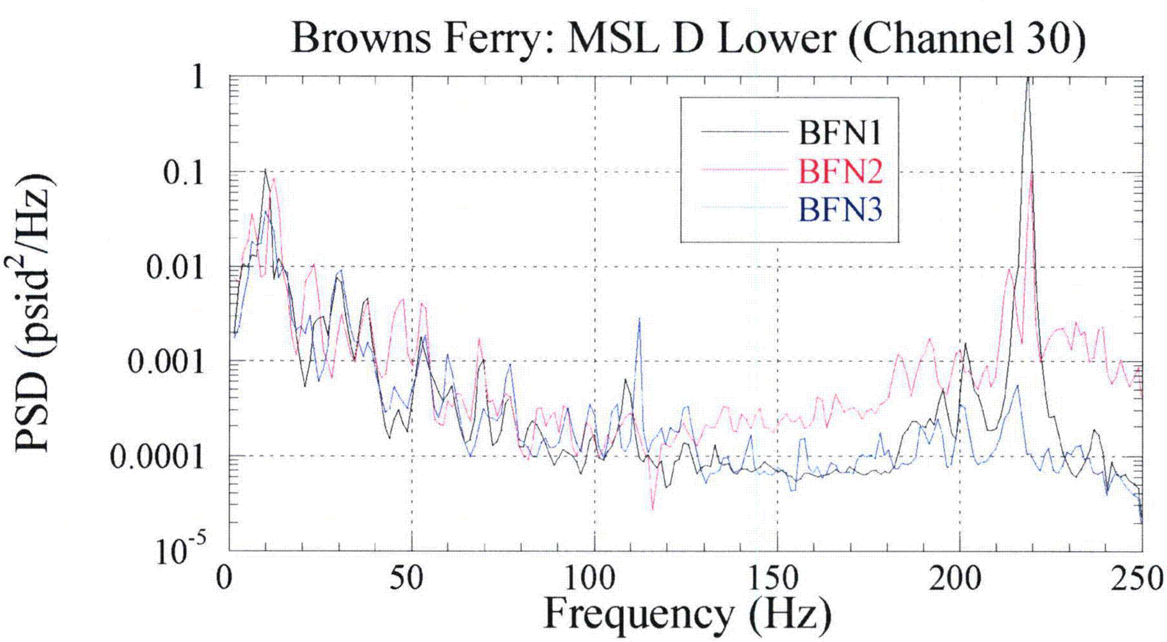

Figure EMCB.151-5: PSD comparison of pressure measurements on MSLs

NRC RAI EMCB.193/152 (Unit 1/Unit 2)

TVA presents the stress analyses of Unit 1 and Unit 2 steam dryer in CDI reports 08-15P and 08-16P, respectively. In these reports, TVA has proposed several structural modifications to increase the alternating stress ratio. Describe the inspections that will be performed during the installation of the modifications. Specifically, confirm whether the root pass of the welds will be inspected. Additionally provide confirmation whether any local stress relief heat treatment will be provided to the welds.

TVA Response to EMCB.193/152 (Unit 1/Unit 2)

During the initial Unit 1 dryer structural modifications the following base metal and welding inspections were performed:

- Visually inspected the area where component parts were to be installed
- Interference removal in the area of parts installation was performed with plasma cutting or grinding techniques. VT exams of cut or ground areas for linear defects within 2 inches of the final prep area were performed. Acceptance criteria for base metal areas requiring VT exams follow: 1) any linear imperfection grater than 1/16 - inch shall be rejected, 2) any porosity in excess of 3/16-inch in diameter shall be removed, 3) any presence of laminations shall be reported for engineering evaluation
- Final welds were cleaned free from slag, brushed and VT-1 examined

The dryer structural modifications are made in an underwater environment to control contamination and to reduce personnel dose. As such, the welding is performed with underwater welding procedures. The underwater environment precludes any local stress relief heat treatment for installed welds.

The planned additional modifications for Unit 1 and the modifications planned for Unit 2 will be VT examined consistent with the above. In addition root welds will be brush cleaned and VT examined prior to adding additional weld passes.

ENCLOSURE 3

TENNESSEE VALLEY AUTHORITY
BROWNS FERRY NUCLEAR PLANT (BFN)
UNITS 1, 2, AND 3

TECHNICAL SPECIFICATIONS (TS) CHANGES TS-431 AND TS-418
EXTENDED POWER UPRATE (EPU)

AFFIDAVIT

Attached is the CDI affidavit for the proprietary information contained in Enclosure 1.

Continuum Dynamics, Inc.

(609) 538-0444 (609) 538-0464 fax 34 Lexington Avenue Ewing, NJ 08618-2302

AFFIDAVIT

Re: Browns Ferry Nuclear Plant (BFN) – Units 1, 2, and 3 – Technical Specifications (TS) Changes TS-431 and TS-418 – Extended Power Uprate (EPU) – Response to Round 19 Request for Additional Information (RAI) (TAC Nos. MD5262, MD5263 and MD5264)

I, Milton E. Teske, being duly sworn, depose and state as follows:

1. I hold the position of Senior Associate of Continuum Dynamics, Inc. (hereinafter referred to as C.D.I.), and I am authorized to make the request for withholding from Public Record the Information contained in the documents described in Paragraph 2. This Affidavit is submitted to the Nuclear Regulatory Commission (NRC) pursuant to 10 CFR 2.390(a)(4) based on the fact that the attached information consists of trade secret(s) of C.D.I. and that the NRC will receive the information from C.D.I. under privilege and in confidence.

2. The Information sought to be withheld, as transmitted to TVA Browns Ferry as attachment to C.D.I. Letter No. 08149 dated 29 August 2008 Browns Ferry Nuclear Plant (BFN) – Units 1, 2, and 3 – Technical Specifications (TS) Changes TS-431 and TS-418 – Extended Power Uprate (EPU) – Response to Round 19 Request for Additional Information (RAI) (TAC Nos. MD5262, MD5263 and MD5264).

3. The Information summarizes:

   (a) a process or method, including supporting data and analysis, where prevention of its use by C.D.I.'s competitors without license from C.D.I. constitutes a competitive advantage over other companies;
   (b) Information which, if used by a competitor, would reduce his expenditure of resources or improve his competitive position in the design, manufacture, shipment, installation, assurance of quality, or licensing of a similar product;
   (c) Information which discloses patentable subject matter for which it may be desirable to obtain patent protection.

   The information sought to be withheld is considered to be proprietary for the reasons set forth in paragraphs 3(a), 3(b) and 3(c) above.

4. The Information has been held in confidence by C.D.I., its owner. The Information has consistently been held in confidence by C.D.I. and no public disclosure has been made and it is not available to the public. All disclosures to third parties, which have been limited, have been made pursuant to the terms and conditions contained in C.D.I.'s Nondisclosure Secrecy Agreement which must be fully executed prior to disclosure.

5. The Information is a type customarily held in confidence by C.D.I. and there is a rational basis therefore. The Information is a type, which C.D.I. considers trade secret and is held in confidence by C.D.I. because it constitutes a source of competitive advantage in the competition and performance of such work in the industry. Public disclosure of the Information is likely to cause substantial harm to C.D.I.'s competitive position and foreclose or reduce the availability of profit-making opportunities.

I declare under penalty of perjury that the foregoing affidavit and the matters stated therein are true and correct to be the best of my knowledge, information and belief.

Executed on this 29 day of August 2008.

Milton E. Teske
Continuum Dynamics, Inc.

Subscribed and sworn before me this day: August 29, 2008

Eileen P. Burmeister

Eileen P. Burmeister, Notary Public

EILEEN P. BURMEISTER
NOTARY PUBLIC OF NEW JERSEY
MY COMM. EXPIRES MAY 6, 2012